Flow cytometry

Spleen and LN cells were stained with fluorescein isothiocyanate (FITC)-conjugated anti-CD8, phycoerythrin (PE)-conjugated anti-CD4, PE-Cy5.5-conjugated anti-CD44, APC-conjugated anti-CD62L, FITC-conjugated anti-CD5, APC-conjugated anti-CD27, PE-conjugated anti-B220, PE-Cy7-conjugated anti-CD19-C, PE-conjugated anti-TRAIL mAb (eBiosciences, San Diego, CA, USA). Cells were analyzed by a FACScan (BD Biosciences, Franklin Lakes, NJ, USA).

Proliferation assay

T cells (>90%) were enriched from single-cell suspensions of spleen and ILN cells from recipient MRL/*lpr* mice with nylon wool (Wako Pure Chemical, Tokyo, Japan), and $CD4^+$ T cells were purified by Phycoerythrin (PE)-conjugated anti-CD4 mAb, PE-conjugated CD8 mAb, and anti-PE Microbeads (Miltenyi Biotec). Cells were cultured in 96-well flat-bottom microtiter plates (5×10^4 cells/well) in RPMI1640 containing 10% FCS, penicillin/streptomycin, and 2-mercaptoethanol (ME), and were stimulated with plate-coated anti-CD3 (500A2) (BD Biosciences) and anti-CD28 mAb (37.51) (BD Biosciences). [^{3}H]Thymidine incorporation during the last 12 hours of the culture for 72 hours was evaluated using an automated β liquid scintillation counter. In addition, cells were labeled with carboxyfluorescein diacetate succinimidyl ester (CFSE), and dilution of CFSE was evaluated as cell proliferation after stimulation by flow cytometric analysis.

ELISA

The amounts of mouse IL-2, IFN-γ, IL-4, IL-10, and IL-17 in culture supernatants, rheumatoid factor (RF) (IgM and IgG), anti-double strand (ds)DNA, anti-CII, and anti-nuclear Ab (ANA) (ALPHA DIAGNOSTIC INTERNATIONAL) of sera from the recipient MRL/*lpr* mice were detected by ELISA as previously described [14].

Detection of apoptotic cells

To determine the apoptosis of T and B cells by repeated interactions with DCs, T and B cells were co-cultured for 8 hours three times with RANKL-stimulated MRL/*lpr* or MRL+/+ BMDCs. Briefly, we transferred T cells into the other well, in which DCs had been stimulated, without interval three times for each 8 hours. After the third co-culture with DCs, apoptotic cells of $CD4^+$, $CD8^+$ T, DNT, and B cells were detected with flow cytometer using an Annexin V-FITC apoptosis detection kit (Bio Vision, Mountain View, CA). Purified anti-mouse TRAIL mAb (BioLegend, San Diego, CA, clone:N2B2) was used for inhibition of T cell apoptosis.

Gene expression analysis

Apoptosis pathway-focused gene expression profiling analysis using real-time polymerase chain reaction (PCR) was tested with a PCR Primer array kit (SABiosciences Corporation, Frederick, MD, USA). In brief, total RNA was extracted with RNeasy kits (Qiagen Inc., Valencia, CA), and reverse transcribed. The synthesized cDNA was then applied to PCR-based SuperArray (SABiosciences) plates to detect expression of genes related to apoptosis using a PTC-200 DNA Engine Cycler (BioRad Kaboratories, Hercules, CA) with SYBR Premix Ex Taq (Takara, Kyoto, Japan).

Real-time quantitative reverse transcription-polymerase chain reaction (RT-PCR)

Total RNA was extracted from the cultured $CD4^+$ T cells of MRL/*lpr* mice using RNeasy kits (Qiagen), and reverse-transcribed. Transcript levels of TRAF3, caspase 8, Tnfrsf10b (TRAIL-R2), Bcl-2, and β-actin were observed using PTC-200 DNA Engine Cycler (BioRad) with SYBR Premix Ex Taq (Takara, Kyoto, Japan). The following primer sequences were used: for TRAF3, 5′-AGCAGCTGACTCTGGGACAT-3′ (forward) and 5′-CACCACACAGGGACAATCTG-3′ (reverse); for Tnfrsf10b (TRAIL-R2), 5′-ACTTGCTGAGAGCTGACTCTGTGG-3′ (forward) and 5′-AGCAGTGGCTGTGTTCACAAGG-3′ (reverse); for caspase 8, 5′-GAGATCCTGTGAATGGAACCTGGTA-3′ (forward) and 5′-CACGCCAGTCAGGATGCTAAGA-3′ (reverse); for Bcl-2, 5′-TTCGCAGCGATGTCCAGTCAGC-3′ (forward) and 5′-TGAAGAGTTCTTCCACCACCGT-3′ (reverse); and for β-actin, 5′-GTGGGCCGCTCTAGGCACCA-3′ (forward) and 5′-CGGTTGGCCTTAGGGTTCAGGGGGG-3′ (reverse). Relative mRNA abundance of each transcript was normalized against β-actin.

In vitro knockdown of TRAIL gene in BMDCs

Small interfering RNA (siRNA) of TRAIL (Tnfs10) and a negative control (Stealth™ Select RNAi, Cat No:10620319, Invitrogen, Carlsbad, CA, USA), including three sequences as off-targets were used for analysis of *in vitro* knockdown of TRAIL gene in RANKL-stimulated DCs. Transfection of siRNA into DCs was performed with Lipofectamine™ RNAiMAX Reagent (Invitrogen).

Statistical Analysis

Results are given as mean ± standard deviation (SD). Comparison was done using Student's *t* test. Differences were considered statistically significant for *P* values of <0.05.

Supporting Information

Figure S1 The effect of multiple transfers of activated *lpr* DCs on RA lesion and autoantibody production in MRL/*lpr* mice. (A) RA lesions of recipient female mice treated with multiple transfers of DCs that were stimulated by different condition in vitro were compared. The histological score of the recipient mice (16 weeks of age) was evaluated at 12 weeks after repeated transfers. Data are shown as means ± SD (n = 5 per group respectively). (B) Autoantibody production of anti-dsDNA, anti-CII, and anti-nuclear Ab (ANA) of the sera from non-treated, stimulated +/+ DC-transferred, and stimulated *lpr* DC-transferred mice (16 weeks of age) was measured by ELISA. Data are shown as means ± SD (n = 5 per group respectively). (C) Autoantibody production of anti-dsDNA and anti-CII Abs of the sera from mice (16 weeks of age) transferred with RANKL, or RANKL and CII-stimulated *lpr* DCs was measured by ELISA. Data are shown as means ± SD (n = 5 per group respectively). *$p<0.05$.
(TIF)

Figure S2 Apoptosis of T and B cells by multiple transfers of *lpr* DCs. Apoptosis (annexin V^+) of $CD4^+$ (A), $CD8^+$ (B) T, DNT (C), and B ($CD19^+$) (D) cells of spleen and ILNs in the recipient mice was detected by flow cytometric analysis at 2 weeks after the multiple transfers. Data are shown as means ± SD (n = 3 per group respectively). *$p<0.05$, **$p<0.005$.
(TIF)

Figure S3 Activation or maturation markers on T and B cells. (A) T cell markers (CD44 and CD62L) of $CD4^+$-gated cells of spleen and ILNs in the recipients (16 weeks of age) were analyzed by flow cytometry at 12 weeks after the multiple transfers. Results were representative of 5 mice per group. (B) B cell markers (CD27 and CD5) of $CD19^+$-gated cells of spleen and ILNs in the recipients were analyzed by flow cytometry at 12 weeks after the multiple transfers. Results were representative of 5 mice per group.
(TIF)

Figure S4 Survival of DCs in MRL/*lpr* mice. BMDCs from MRL+/+ or MRL/lpr mice were stimulated with or without RANKL and CII, and then were labeled with CFSE. Those DCs were subcutaneously injected into MRL/*lpr* mice. At 2 weeks after the transfer, $CFSE^+CD11C^+$ DCs of ILNs (A) and spleen (B) were detected by flow cytometric analysis. Data are shown as means ± SD (n = 5 per group respectively). *$p<0.05$.
(TIF)

Figure S5 Effect of multiple DC transfer on T cell proliferation in MRL+/+ mice. At 12 weeks after multiple DC transfers into MRL+/+ mice, CFSE-labeled $CD4^+$ T cells were stimulated with anti-CD3 (0.5 μg/ml) and anti-CD28 (10 μg/ml) mAbs for 72 hours. Dilution of CFSE in $CD4^+$ T cells was evaluated as proliferative cells by flow cytometric analysis. Data are shown as means ± SD (n = 5 per group respectively).
(TIF)

Figure S6 Effects of multiple DC transfer on thymic differentiation of T cell and T_{reg} differentiation. (A) T cell phenotype (CD4 and CD8) in the thymus of the recipient mice was analyzed by flow cytometry at 12 weeks after the multiple DC transfer. Results were representative of 5 mice per group. (B) $CD25^+$ $Foxp3^+$ $CD4^+$ T_{reg} cells in ILNs and spleen were detected by flow cytometric analysis. Results were representative of 5 mice per group.
(TIF)

Figure S7 Efficiency of siRNA on TRAIL expression. (A) TRAIL expression on *lpr* BMDCs treated with control or TRAIL siRNA (0, 10 and 50 nM) was detected by flow cytometric analysis. Results were representative of individual three experiments. (B) Relative expression of TRAIL to that of untreated DCs was shown.
(TIF)

Figure S8 Effect of transfer of TRAIL siRNA-treated DCs on autoantibody production. Autoantibodies such as anti-dsDNA and anti-CII Abs of the sera from mice (16 weeks of age) transferred with control and TRAIL siRNA-treated DCs were detected by ELISA. Data are shown as means ± SD (n = 5 per group respectively). *$p<0.05$.
(TIF)

Acknowledgments

We thank Ai Katayama, Noriko Kino, Satoko Katada, and Akihiko Yoshida for their technical assistance.

Author Contributions

Conceived and designed the experiments: TI NI ET YH. Performed the experiments: TI NI RO KM TK MK YK. Analyzed the data: TI NI AY RA. Wrote the paper: TI NI YH.

References

1. Firestein GS (2003) Evolving concepts of rheumatoid arthritis. Nature 423: 356–361.
2. McInnes IB, Schett G (2007) Cytokines in the pathogenesis of rheumatoid arthritis. Nat Rev Immunol 7: 429–442.
3. Takayanagi H (2007) Osteoimmunology: shared mechanisms and crosstalk between the immune and bone systems. Nat Rev Immunol 7: 292–304.
4. Merad M, Manz MG (2009) Dendritic cell homeostasis. Blood 113: 3418–3427.
5. Rescigno M, Martino M, Sutherland CL, Gold MR, Ricciardi-Castagnoli P (1998) Dendritic cell survival and maturation are regulated by different signaling pathways. J Exp Med 188: 2175–2180.
6. Yamamoto M, Sato S, Hemmi H, Sanjo H, Uematsu S, et al. (2002) Essential role for TIRAP in activation of the signalling cascade shared by TLR2 and TLR4. Nature 420: 324–329.
7. Anderson DM, Maraskovsky E, Billingsley WL, Dougall WC, Tometsko ME, et al. (1997) A homologue of the TNF receptor and its ligand enhance T-cell growth and dendritic-cell function. Nature 390: 175–179.
8. Caux C, Massacrier C, Vanbervliet B, Dubois B, Van Kooten, et al. (1994) Activation of human dendritic cells through CD40 cross-linking. J Exp Med 180: 1263–1272.
9. Van Kooten C, Banchereau J (1997) Functions of CD40 on B cells, dendritic cells and other cells. Curr Opin Immunol 9: 330–337.
10. Van Gool SW, Vandenberghe P, de Boer M, Ceuppens JL (1996) CD80, CD86 and CD40 provide accessory signals in a multiple-step T-cell activation model. Immunol Rev 153: 47–83.
11. Banchereau J, Steinman RM (1998) Dendritic cells and the control of immunity. Nature 392: 245–252.
12. van Duivenvoorde LM, van Mierlo GJ, Boonman ZF, Toes RE (2006) Dendritic cells: vehicles for tolerance induction and prevention of autoimmune diseases. Immunobiology 211: 627–632.
13. Wenink MH, Han W, Toes RE, Radstake TR (2009) Dendritic cells and their potential implication in pathology and treatment of rheumatoid arthritis. Handb Exp Pharmacol 81–98.
14. Izawa T, Ishimaru N, Moriyama K, Kohashi M, Arakaki R, et al. (2007) Crosstalk between RANKL and Fas signaling in dendritic cells controls immune tolerance. Blood 110: 242–50.
15. Wong BR, Josien R, Choi Y (1999) TRANCE is a TNF family member that regulates dendritic cell and osteoclast function. J Leukoc Biol 65: 715–24.
16. Yasuda H, Shima N, Nakagawa N, Yamaguchi K, Kinosaki M, et al. (1998) Osteoclast differentiation factor is a ligand for osteoprotegerin/osteoclastogenesis-inhibitory factor and is identical to TRANCE/RANKL. Proc Natl Acad Sci U S A 95: 3597–3602.
17. Lacey DL, Timms E, Tan HL, Kelley MJ, Dunstan CR, et al. (1998) Osteoprotegerin ligand is a cytokine that regulates osteoclast differentiation and activation. Cell 93: 165–176.
18. Simonet WS, Lacey DL, Dunstan CR, Kelley M, Chang MS, et al. (1997) Osteoprotegerin: a novel secreted protein involved in the regulation of bone density. Cell 89: 309–319.
19. Shalhoub V, Elliott G, Chiu L, Manoukian R, Kelley M, et al. (2000) Characterization of osteoclast precursors in human blood. Br J Haematol 111: 501–512.
20. Kong YY, Yoshida H, Sarosi I, Tan HL, Timms E, et al. (1999) OPGL is a key regulator of osteoclastogenesis, lymphocyte development and lymph-node organogenesis. Nature 397: 315–323.
21. Fata JE, Kong YY, Li J, Sasaki T, Irie-Sasaki J, et al. (2000) The osteoclast differentiation factor osteoprotegerin-ligand is essential for mammary gland development. Cell 103: 41–50.
22. Plows D, Kontogeorgos G, Kollias G (1999) Mice lacking mature T and B lymphocytes develop arthritic lesions after immunization with type II collagen. J Immunol 162: 1018–1023.
23. Bonardelle D, Bobé P, Reynès M, Amouroux J, Tricottet V, et al. (2001) Inflammatory arthropathy in MRL hematopoietic chimeras undergoing Fas mediated graft-versus-host syndrome. J Rheumatol 28: 956–961.
24. Edwards CK 3rd, Zhou T, Zhang J, Baker TJ, De M, et al. (1996) Inhibition of superantigen-induced proinflammatory cytokine production and inflammatory arthritis in MRL-lpr/lpr mice by a transcriptional inhibitor of TNF-alpha. J Immunol 157: 1758–1772.
25. Watanabe-Fukunaga R, Brannan CI, Copeland NG, Jenkins NA, Nagata S (1992) Lymphoproliferation disorder in mice explained by defects in Fas antigen that mediates apoptosis. Nature 356: 314–317.
26. Morse HC 3rd, Davidson WF, Yetter RA, Murphy ED, Roths JB, et al (1982) Abnormalities induced by the mutant gene Ipr: expansion of a unique lymphocyte subset. J Immunol 129: 2612–2615.
27. Zhang XR, Zhang LY, Devadas S, Li L, Keegan AD, et al. (2003) Reciprocal expression of TRAIL and CD95L in Th1 and Th2 cells: role of apoptosis in T helper subset differentiation. Cell Death Differ 10: 203–210.
28. Fanger NA, Maliszewski CR, Schooley K, Griffith TS (1999) Human dendritic cells mediate cellular apoptosis via tumor necrosis factor-related apoptosis-inducing ligand (TRAIL). J Exp Med 190: 1155–1164.

29. Jeremias I, Herr I, Boehler T, Debatin KM (1998) TRAIL/Apo-2-ligand-induced apoptosis in human T cells. Eur J Immunol 28: 143–152.
30. Sarkar S, Fox DA (2005) Dendritic cells in rheumatoid arthritis. Front Biosci 10: 656–665.
31. Elliot MJ, Maini RN, Feldmann M, Long-Fox A, Charles P, et al. (2008) Treatment of rheumatoid arthritis with chimeric monoclonal antibodies to tumor necrosis factor alpha. Arthritis Rheum 58: S92–S101.
32. Menges M, Rossner S, Voigtlander C, Schindler H, Kukutsch NA, et al. (2002) Repetitive injections of dendritic cells matured with tumor necrosis factor alpha induce antigen-specific protection of mice from autoimmunity. J Exp Med 195: 15–21.
33. Lopatin U, Yao X, Williams RK, Bleesing JJ, Dale JK, et al. (2001) Increases in circulating and lymphoid tissue interleukin-10 in autoimmune lymphoproliferative syndrome are associated with disease expression. Blood 97: 3161–3170.
34. Prud'homme GJ, Kono DH, Theofilopoulos AN (1995) Quantitative polymerase chain reaction analysis reveals marked overexpression of interleukin-1 beta, interleukin-1 and interferon-gamma mRNA in the lymph nodes of lupus-prone mice. Mol Immunol 32: 495–503.
35. Llorente L, Zou W, Levy Y, Richaud-Patin Y, Wijdenes J, et al. (1995) Role of interleukin 10 in the B lymphocyte hyperactivity and autoantibody production of human systemic lupus erythematosus. J Exp Med 181: 839–44.
36. Houssiau FA, Lefebvre C, Vanden Berghe M, Lambert M, Devogelaer JP, et al. (1995) Serum interleukin 10 titers in systemic lupus erythematosus reflect disease activity. Lupus 4: 393–395.
37. Wu X, Pan G, Mckenna MA, Zayzafoon M, Xiong WC, et al. (2005) RANKL regulates Fas expression and Fas-mediated apoptosis in osteoclasts. J Bone Miner Res 20: 107–116.
38. Pan G, Ni J, Wei YF, Yu G, Gentz R, et al. (1997) An antagonist decoy receptor and a death domain-containing receptor for TRAIL. Science 277: 815–818.
39. Schneider P, Bodmer JL, Thome M, Hofmann K, Holler N, et al. (1997) Characterization of two receptors for TRAIL. FEBS Lett 416: 329–334.
40. Sheikh MS, Huang Y, Fernandez-Salas EA, El-Deiry WS, Friess H, et al. (1999) The antiapoptotic decoy receptor TRID/TRAIL-R3 is a p53-regulated DNA damage-inducible gene that is overexpressed in primary tumors of the gastrointestinal tract. Oncogene 18: 4153–4159.
41. Sheridan JP, Marsters SA, Pitti RM, Gurney A, Skubatch M, et al. (1997) Control of TRAIL-induced apoptosis by a family of signaling and decoy receptors. Science 277: 818–821.
42. Sprick MR, Rieser E, Stahl H, Grosse-Wilde A, Weigand MA, et al. (2002) Caspase-10 is recruited to and activated at the native TRAIL and CD95 death-inducing signalling complexes in a FADD-dependent manner but can not functionally substitute caspase-8. Embo J 21: 4520–4530.
43. Bodmer JL, Holler N, Reynard S, Vinciguerra P, Schneider P, et al. (2000) TRAIL receptor-2 signals apoptosis through FADD and caspase-8. Nat Cell Biol 2: 241–243.
44. Hersey P, Zhang XD (2001) How melanoma cells evade trail-induced apoptosis. Nat Rev Cancer 1: 142–150.
45. Liu Z, Xu X, Hsu HC, Tousson A, Yang PA, et al. (2003) CII-DC-AdTRAIL cell gene therapy inhibits infiltration of CII-reactive T cells and CII-induced arthritis. J Clin Invest 112: 1332–1341.
46. Krammer PH, Arnold R, Lavrik IN (2007) Life and death in peripheral T cells. Nat Rev Immunol 7: 532–542.
47. Russell JH, Ley TJ (2002) Lymphocyte-mediated cytotoxicity. Annu Rev Immunol 20: 323–370.
48. Lamhamedi-Cherradi SE, Zheng SJ, Maguschak KA, Peschon J, Chen YH (2003) Defective thymocyte apoptosis and accelerated autoimmune diseases in TRAIL-/- mice. Nat Immunol 4: 255–260.
49. Inaba K, Inaba M, Romani N, Aya H, Deguchi M, et al. (1992) Generation of large numbers of dendritic cells from mouse bone marrow cultures supplemented with granulocyte/macrophage colony-stimulating factor. J Exp Med 176: 1693–1702.
50. Andrews BS, Eisenberg RA, Theofilopoulos AN, Izui S, Wilson CB, et al. (1978) Spontaneous murine lupus-like syndromes. Clinical and immunopathological manifestations in several strains. J Exp Med 148: 1198–1215.
51. Hang L, Theofilopoulos AN, Dixon FJ (1982) A spontaneous rheumatoid arthritis-like disease in MRL/l mice. J Exp Med 155: 1690–1701.
52. O'Sullivan FX, Fassbender HG, Gay S, Koopman WJ (1985) Etiopathogenesis of the rheumatoid arthritis-like disease in MRL/l mice. I. The histomorphologic basis of joint destruction. Arthritis Rheum 28(5): 529–536.
53. Tarkowski A, Jonsson R, Holmdahl R, Klareskog L (1987) Immunohistochemical characterization of synovial cells in arthritic MRL-lpr/lpr mice. Arthritis Rheum 30: 75–82.

THE JOURNAL OF IMMUNOLOGY

Induction of Rapid T Cell Death and Phagocytic Activity by Fas-Deficient *lpr* Macrophages

Ritsuko Oura, Rieko Arakaki, Akiko Yamada, Yasusei Kudo, Eiji Tanaka, Yoshio Hayashi and Naozumi Ishimaru

J Immunol 2013; 190:578-585; Prepublished online 19 December 2012;
doi: 10.4049/jimmunol.1103794
http://www.jimmunol.org/content/190/2/578

The Journal of Immunology is published twice each month by The American Association of Immunologists, Inc., 9650 Rockville Pike, Bethesda, MD 20814-3994.

Print ISSN: 0022-1767 Online ISSN: 1550-6606.

Induction of Rapid T Cell Death and Phagocytic Activity by Fas-Deficient *lpr* Macrophages

Ritsuko Oura,*,† Rieko Arakaki,* Akiko Yamada,* Yasusei Kudo,* Eiji Tanaka,† Yoshio Hayashi,* and Naozumi Ishimaru*

Peripheral T cells are maintained by the apoptosis of activated T cells through the Fas–Fas ligand system. Although it is well known that normal T cells fail to survive in the Fas-deficient immune condition, the molecular mechanism for the phenomenon has yet to be elucidated. In this study, we demonstrate that rapid cell death and clearance of normal T cells were induced by Fas-deficient *lpr* macrophages. Transfer of normal T cells into *lpr* mice revealed that Fas expression on donor T cells was promptly enhanced through the IFN-γ/IFN-γR. In addition, Fas ligand expression and phagocytic activity of *lpr* macrophages were promoted through increased NF-κB activation. Controlling Fas expression on macrophages plays an essential role in maintaining T cell homeostasis in the peripheral immune system. Our data suggest a critical implication to the therapeutic strategies such as transplantation and immunotherapy for immune disorder or autoimmunity related to abnormal Fas expression. *The Journal of Immunology*, **2013, 190: 578–585.**

The Fas receptor is expressed on most tissues and plays an important role in regulating the normal function of many different organs. Fas signaling can regulate T cell and B cell differentiation, maturation, activation, and deletion in the peripheral immune system (1–3). Activation-induced cell death (AICD) is involved in the removal of activated T cells in vivo and depends on Fas and Fas ligand (FasL) (4, 5). Among apoptotic mechanisms, AICD plays a central role in the removal of autoreactive T cells and in prevention of autoimmune responses (6).

MRL/Mp mice bearing a Fas deletion mutant gene, *lpr* (MRL/*lpr*), spontaneously develop autoimmune lesions resembling human glomerulonephritis, arthritis, vasculitis, and Sjögren's syndrome (7–10). In addition, *gld* mice defective in the FasL gene exhibit autoimmune lesions (11). Both strains lack the cell death mechanism mediated through the Fas–FasL interaction in the immune system. Ligation of Fas by the homotrimeric FasL results in the clustering of Fas and recruitment of the adaptor protein Fas-associated death domain to clustered Fas intracellular death domains (5, 12–14). In addition, Fas and only the Bcl2 homology domain 3 (BH3-only protein) such as Bim play overlapping roles in peripheral T cell death in immune response shutdown and prevention of immune disorders (15). In contrast, the regulation of T cell susceptibility to AICD is controlled by T cell maturity and activation and the presence or absence of APCs such as macrophages or dendritic cells (5, 16).

Normal hematopoietic cells including spleen and bone marrow cells do not survive in *lpr* mice (17, 18). In addition, it was reported that in vitro coculture of normal and *lpr*-derived T cell lines resulted in the loss of the normal T cells (17, 19). These in vivo and in vitro findings could be explained by the elevated FasL expression on *lpr* immune cells (20, 21). However, the precise mechanism underlying the FasL overexpression in *lpr* immune cells or the association of normal T cell deletion with APCs in Fas-deficient *lpr* mice remains unclear.

In this study, we focused on T cell apoptosis in Fas-deficient recipients using C57BL/6/*lpr* mice to define the cellular and molecular mechanisms of AICD in T cells and the regulation of FasL expression. Furthermore, we investigated whether macrophages in Fas-deficient *lpr* mice contribute to the clearance of apoptotic T cells in the peripheral immune system.

Materials and Methods

Mice

C57BL/6 (B6), B6-*lpr*/*lpr* (B6/*lpr*), and B6-*gld*/*gld* (B6/*gld*) mice were purchased from Japan SLC Laboratory (Shizuoka, Japan). OT-II mice (C57BL/6-Tg (TcraTcrb) 425Cbn/J) and IFN-γR gene knockout ($IFN\gamma R^{-/-}$) mice were obtained from Dr. J. Sprent. $NF\text{-}\kappa B_1^{-/-}$ mice were obtained from The Jackson Laboratory. GFP-transgenic (TG) mice were obtained from RIKEN BioResource Center (Tsukuba, Japan). All mice were bred at the animal facility of the University of Tokushima under specific pathogen-free conditions. The experiments were approved by an animal ethics board of the University of Tokushima.

Adoptive cell transfer

T cells were purified from the spleen of B6, GFP-TG, OT-II, B6/*lpr*, or $IFN\gamma R^{-/-}$ mice using Abs including anti-MHC class II, anti-B220 (eBioscience, San Diego, CA), and immunomagnetic beads (Dynal, Oslo, Norway). T cells from all mice, except GFP-TG mice, were labeled with CFSE (Invitrogen, Carlsbad, CA). A total of 1, 2, or 5×10^6 T cells were i.v. or i.p. transferred into B6, B6/*lpr*, B6/*gld*, or $NF\text{-}\kappa B_1^{-/-}$/*lpr* mice. For homeostatic expansion, the recipient mice were irradiated at 8.5

*Department of Oral Molecular Pathology, Institute of Health Biosciences, University of Tokushima Graduate School, Tokushima 770-8504, Japan; and †Department of Orthodontics and Dentofacial Orthopedics, Institute of Health Biosciences, University of Tokushima Graduate School, Tokushima 770-8504, Japan

Received for publication December 28, 2011. Accepted for publication November 12, 2012.

This work was supported by the Funding Program for Next Generation World-Leading Researchers in Japan (Grant LS090) and by Grants-in-Aid for Scientific Research (17109016 and 17689049) from the Ministry of Education, Science, Sport and Culture of Japan.

Address correspondence and reprint requests to Dr. Naozumi Ishimaru, Department of Oral Molecular Pathology, Institute of Health Biosciences, University of Tokushima Graduate School, 3-18-15 Kuramotocho, Tokushima 770-8504, Japan. E-mail address: ishimaru@dent.tokushima-u.ac.jp

The online version of this article contains supplemental material.

Abbreviations used in this article: AICD, activation-induced cell death; B6, C57BL/6; B6/*gld*, C57BL/6-*gld*/*gld*; B6/*lpr*, C57BL/6-*lpr*/*lpr*; FasL, Fas ligand; $IFN\gamma R^{-/-}$, IFN-γR gene knockout; LN, lymph node; PEC, peritoneal exudate cell; TG, transgenic.

www.jimmunol.org/cgi/doi/10.4049/jimmunol.1103794

Gy before T cell transfer. For the analysis of donor T cells, spleen cells, lymph node (LN) cells, PBMCs, or peritoneal exudate cells (PECs) were analyzed by flow cytometry. To inhibit in vivo deletion of T cells, anti-FasL mAb (clone MFL3; BioLegend, San Diego, CA) was i.p. injected into recipient mice together with transfer of T cells.

Flow cytometry

FITC, PE, allophycocyanin–peridin chlorophyll protein, PE-Cy5.5, PE-Cy7, or allophycocyanin–Cy7-conjugated Abs including anti-CD4, CD8, CD11b, Fas, and FasL Abs, were used. A FACScan flow cytometer (BD Biosciences, Franklin Lakes, NJ) was used, and data were analyzed using the FlowJo FACS Analysis software (Tree Star, Ashland, OR).

In vivo imaging

The mice were s.c. injected with isoflurane (Abbott Laboratories, Abbot Park, IL) as an anesthetic. Purified T cells were incubated with XenoLight DiR (Caliper Life Sciences, Hopkinton, MA) for 30 min. A total of 5×10^6 T cells were i.v. transferred into recipient mice, and donor T cells were monitored at 30 min, 2 h, and 6 h using in vivo imaging analyzer (Caliper Life Sciences).

ELISA

The concentration of IFN-γ in sera was measured by ELISA. Ninety-six-well flat-bottom plates were precoated with capture Abs, and diluted samples or standard recombinant cytokines were added to each well. After the plates were washed, biotinylated Abs were added, and the wells were incubated with HRP-labeled, affinity-purified anti-rat IgG. A solution of *o*-phenylenediamine (Sigma-Aldrich, St. Louis, MO) was added to each well as the substrate. The optimal density at 490 nm was measured using a microplate reader (Model 680; Bio-Rad Laboratories, Richmond, CA).

Quantitative RT-PCR

Total RNA was extracted from spleen cells or PECs using Isogen (Wako Pure Chemical Industries, Osaka, Japan); it was then reverse transcribed. The transcript levels of FasL, TNF-α, IL-6, IL-1β, and β-actin were performed using a PTC-200 DNA Engine Cycler (Bio-Rad Laboratories) with SYBR Premix Ex Taq (Takara Bio, Shiga, Japan). The primer sequences used were as follows: FasL, forward, 5′-GTGGGCCGCTCTAGGCACCA-3′, and reverse, 5′-CGGTTGGCCTTAGGGTTCAGGGGG-3′; TNF-α, forward, 5′-ATGAGCACAGAAAGCATGATC-3′, and reverse, 5′-AGATGATCTGAGTGTGAGGG-3′; IL-6, forward, 5′-CTCTGCAAGAGACTTCCAT-3′, and reverse, 5′-ATAGGCAAATTTCCTGATTATA-3′; IL-1β, forward, 5′-TGATGAGAATGACCTGTTCT-3′, and reverse, 5′-CTTCTTCAAAGATGAAGGAAA-3′; β-actin, forward, 5′-GTGGGCCGCTCTAGGCACCA-3′, and reverse, 5′-CGGTTGGCCTTAGGGTTCAGGGGG-3′.

Preparation of peritoneal macrophages

Mice were i.p. injected with 1 ml 3% thioglycollate broth (Sigma-Aldrich), and after 3 or 4 d, elicited macrophages were collected by peritoneal lavage with 5 ml ice-cold PBS.

Phagocytosis assay

Phagocytosis was assessed using Fluoresbrite Yellow Green Caboxylate Microspheres (Polysciences, Warrington, PA). Briefly, the $CD11b^+$ cells purified from PECs were incubated with opsonized beads for 30 min at 37°C and washed with PBS. The phagocytic activity of $CD11b^+$ cells was evaluated by flow cytometric analysis.

Apoptosis detection assay

Apoptosis was detected using the Annexin V-FITC apoptosis detection kit (Bio Vision, Mountain View, CA). Briefly, the cells were washed with PBS and incubated with FITC-conjugated annexin V and propidium iodide for 15 min at room temperature in the dark. Binding buffer was added, and apoptotic cells were detected by flow cytometoric analysis. To inhibit in vitro T cell apoptosis cocultured with PECs, PECs were treated with a Fas-Fc fusion protein (R&D Systems, Minneapolis, MN).

Confocal microscopic analysis

PECs including GFP^+ T cells were stained with PE-conjugated anti-CD11b mAb (eBioscience) on a glass slide. Coverslips were applied with Fluoromount-G (Molecular Probe). Cells were visualized using a Confocal Laser Microscan (LSM 5 Pascal; Carl Zeiss, Oberkochen, Germany).

Western blot analysis

Cell extracts from the nucleus and cytoplasm of $CD11b^+$ PECs were prepared using NE-PER Nuclear and Cytoplasmic Extraction Reagents (Thermo Fisher Scientific, Rockford, IL). A total of 10 μg of each sample per well was used for SDS-PAGE. After blocking with 5% nonfat milk, the membrane was incubated with primary Abs against phospho-IκBα and p50 (NF-κB1), RelA (p65), and histones (Santa Cruz Biotechnology, Santa Cruz, CA). Ag–Ab complexes were detected using HRP-conjugated secondary Abs. Protein binding was visualized using the Phototope-HRP Western blot Detection System (Cell Signaling Technology, Danvers, MA).

NF-κB transcription activity assay

The transcription activity of NF-κB in the nuclear extracts from PECs was analyzed with a NF-κB transcription factor colorimetric assay kit (Millipore, Billerica, MA). Briefly, nuclear extracts were incubated with a biotinylated double-stranded oligonucleotide probe containing the consensus sequence for NF-κB on a streptavidin-coated plate. Captured complexes, including active NF-κB protein, were incubated with the primary Abs for p50 and RelA, HRP-conjugated secondary Ab, and tetramethylbenzidine substrate. The absorbance of the samples was measured using a microplate reader at 450 nm.

Statistical analysis

Statistical significance was determined with an unpaired the Student *t* test.

Results

Normal T cell dynamics in Fas-deficient mice

To understand the dynamics of normal T cells in Fas-deficient mice, the T cells from GFP-TG mice were i.v. transferred into B6 and B6/*lpr* mice. On 7 d after the transfer, GFP^+ cells in the spleen and LNs of the recipient mice were analyzed. Although GFP^+ T cells were found in the spleen and LNs of B6 mice, these cells were barely detectable in B6/*lpr* mice (Fig. 1A). To evaluate the in vivo expansion of normal T cells in Fas-deficient mice using a homeostatic proliferation system, CFSE-labeled normal T cells from B6 mice were i.v. transferred into irradiated B6 and B6/*lpr* mice. On 7 d after the transfer, expanded T cells were found in B6 mice (Fig. 1B). However, the transferred $CFSE^+$ T cells in the spleen and LNs of B6/*lpr* mice were almost undetectable (Fig. 1B). In addition, to examine the in vivo Ag-specific T cell response in B6/*lpr* mice, $CD4^+$ T cells were purified from the spleen of OVA-specific TCR-TG (OT-II) mice and were transferred into B6 and B6/*lpr* mice. OVA peptide (100 μg/mouse) was injected into the recipient mice on the following day. On 7 d after the transfer, OT-II–specific $V\beta5.2^+CD4^+$ T cells of the spleen and LNs were analyzed. Although OT-II T cells were found in the spleen and LNs of B6 recipients, these cells were almost undetectable in the spleen and LNs of B6/*lpr* mice (Fig. 1C). These findings indicate that normal T cells fail to migrate to lymphoid tissues or survive under the Fas-deficient environment. In addition, we examined whether transferred T cells migrate to any specific organ other than lymphoid organs. On 7 d after the transfer of GFP-T cells, T cell diminishment was observed in the spleen, LNs, and liver of B6/*lpr* recipient mice (Fig. 1D). The accumulation of the donor T cells was not observed in any specific organs such as the lung, pancreas, and kidney. Furthermore, the donor T cells did not accumulate in the thymus, bone marrow, and PBMCs of B6/*lpr* recipient mice (Fig. 1D). These findings demonstrate that transferred normal T cells fail to survive in the lymphoid organs such as the spleen and LNs of B6/*lpr* recipients.

Migratory response of normal T cells in Fas-deficient recipients

To examine the migration of normal T cells to lymphoid tissues, in vivo imaging analysis of the dynamics of normal T cells in B6 and B6/*lpr* mice was performed. At 30 min after the transfer of

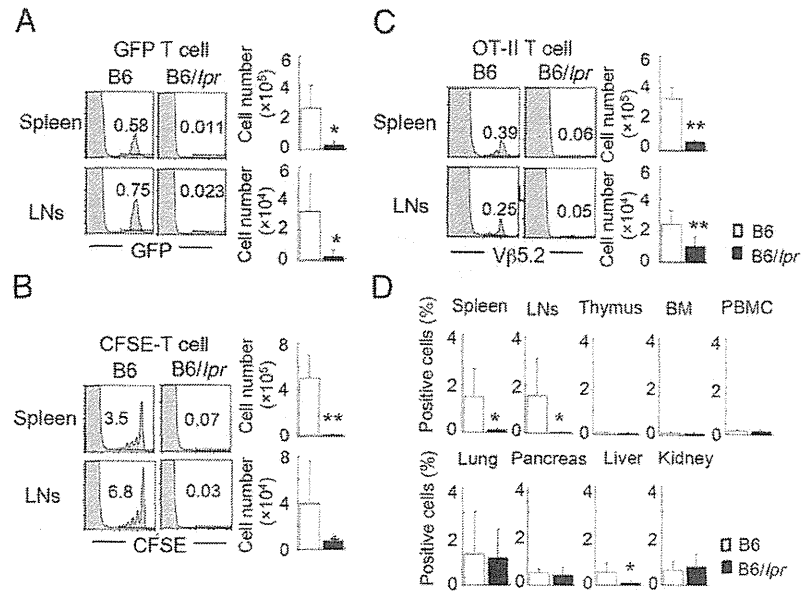

FIGURE 1. Dynamics of normal T cells in B6/*lpr* mice. (**A**) T cells (1×10^6) from GFP-TG mice were transferred into B6 and B6/*lpr* mice. GFP$^+$ T cells in the spleen and LNs of recipient mice at day 7 after the transfer were detected by flow cytometry. (**B**) CFSE-labeled T cells from B6 mice were transferred into irradiated (8.5 Gy) B6 and B6/*lpr* mice. CFSE$^+$ T cells in the spleen and LNs of recipient mice at day 7 after the transfer were detected by flow cytometry. (**C**) T cells (1×10^6) from OT-II mice were transferred into B6 and B6/*lpr* mice. Next day, OVA peptide was i.v. injected into the recipient mice. Vβ5.2$^+$CD4$^+$ T cells in the spleen and LNs of recipient mice at day 7 after the transfer were detected by flow cytometry. Cell numbers were compared between B6 and B6/*lpr* recipients ($n = 6$). (**D**) T cells from GFP-TG mice were transferred into B6 and B6/*lpr* mice. GFP$^+$ T cells in the spleen and LNs of recipient mice at day 7 after the transfer were detected by flow cytometry. GFP$^+$ cells (percentage) were shown as mean ± SD for five mice in each recipient group. $^*p < 0.05$, $^{**}p < 0.005$.

T cells, XenoLight DiR-labeled T cells were detected using an in vivo imaging analyzer. Although transferred T cells were detectable in the spleen of B6 and B6/*lpr* recipients, the fluorescence intensity in the spleen of B6/*lpr* recipients was considerably lower than that in the spleen of B6 recipients (Fig. 2A). This finding suggests that the transferred normal T cells were rapidly diminished in PBMCs before accumulating in lymphoid organs such as the spleen and LNs. In contrast, we have analyzed cell localization to the lung and liver after i.v. injection of T cells. Normal T cells were detectable in both *lpr* and control recipients, and there was no difference in T cell migration between *lpr* and control recipients (Supplemental Fig.1). Moreover, when the transferred T cells (Thy1.1$^+$) were analyzed 30 min after the transfer, the rapid diminishment of T cells in B6/*lpr* recipients had already been observed (Fig. 2B). This suggests that rapid death and clearance of normal T cells may have occurred in the B6/*lpr* recipients immediately after the transfer. Moreover, when the Fas expression on the transferred normal T cells in B6 or B6/*lpr* recipients was analyzed 30 min after the transfer, significantly increased Fas expression was observed on the T cells in B6/*lpr* recipients compared with those in B6 recipients (Fig. 2C). Furthermore, when CFSE-labeled T cells from B6/*lpr* mice were i.v. injected into B6 and B6/*lpr* mice, the T cell diminishment was not detectable in both recipient mice (Fig. 2D). These results suggest that Fas expression on normal T cells plays a crucial role in the induction of rapid T cells diminishment in Fas-deficient recipients. These results imply that Fas-mediated cell death of normal T cells is enhanced in a Fas-deficient immune environment.

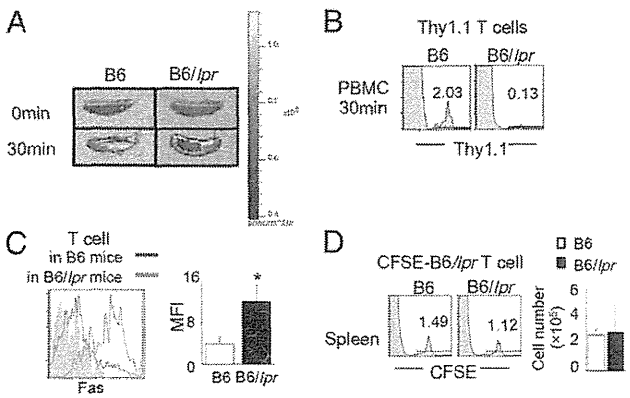

FIGURE 2. Rapid diminishment and Fas expression on the donor T cells in *lpr* recipients. (**A**) T cells (5×10^6) from B6 mice were labeled with XenoLight DiR and transferred into B6 and B6/*lpr* mice. The donor T cells in the spleen of the recipients 30 min after the transfer were detected using an in vivo imaging analyzer. Photos are representative of four mice in each recipient group. (**B**) T cells from B6 Thy1.1 mice were transferred into B6 and B6/*lpr* mice, and the donor T cells in PBMCs of the recipients 30 min after the transfer were detected by flow cytometry. Data are representative of five mice in each recipient group. (**C**) Cell surface Fas expression on the donor T cells in recipients was analyzed 30 min after the transfer by flow cytometry. Mean fluorescence intensity of Fas expression on donor T cells is shown as mean ± SD for five mice in each recipient group. $^*p < 0.05$. (**D**) CFSE-labeled T cells from B6/*lpr* mice were transferred into B6 and B6/*lpr* mice and detected at day 7 after transfer by flow cytometry. Data are representative of five mice in each recipient group.

FasL expression on immune cells in B6/lpr mice

Next, we analyzed FasL expression on peripheral immune cells in B6/*lpr* mice. When mRNA expression of FasL in the spleen of B6 and B6/*lpr* mice was analyzed by quantitative reverse transcription-PCR (RT-PCR), higher levels of FasL mRNA of all subsets including CD4$^+$ T cells, CD8$^+$ T cells, B220$^+$ B cells, CD11c$^+$ dendritic cells, and CD11b$^+$ macrophages were observed in B6/*lpr* mice compared with B6 mice (Fig. 3A). In addition, significantly increased FasL mRNA expression of subsets including CD4$^+$ T cells, CD8$^+$ T cells, and CD11b$^+$ macrophages was observed in PBMCs from B6/*lpr* mice compared with those of B6 mice (Fig. 3B). Therefore, we speculated that FasL–Fas-mediated apoptosis of normal T cells may be induced by the interaction with the peripheral immune cells in B6/*lpr* mice. In particular, because FasL mRNA expression on the CD11b$^+$ macrophages in the spleen and PBMCs of B6/*lpr* mice was much higher than that of B6 mice, macrophages may play a crucial role in T cell apoptosis and clearance in the immune system of B6/*lpr* mice. Thus, we focused on analyzing the macrophages in B6/*lpr* mice. When the surface expression of FasL on macrophages was analyzed by flow cytometry, the expression on the CD11b$^+$ macrophages of the PBMCs of B6/*lpr* mice was increased compared with that of B6 mice (Fig. 3C). These results suggest that increased FasL expressions on immune cells, including macrophages in a Fas-deficient immune condition, play an important

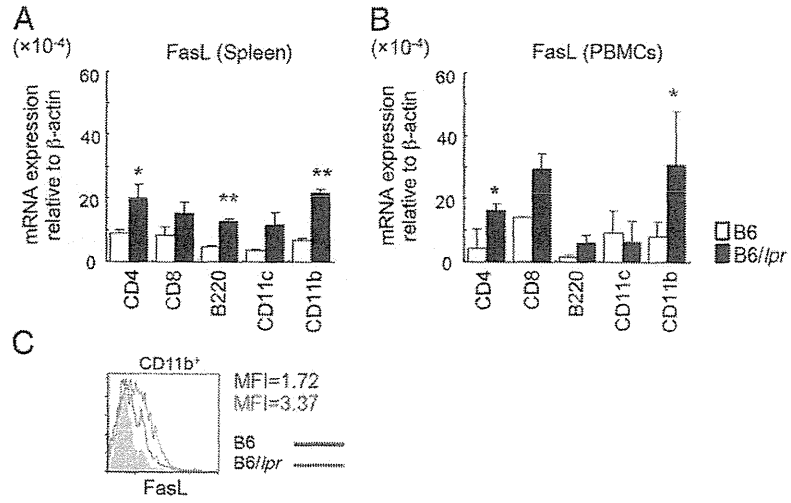

FIGURE 3. Enhanced expression of FasL on the immune cells in B6/*lpr* mice. (**A**) FasL mRNA expressions in spleen cells of B6 and B6/*lpr* mice were analyzed by quantitative RT-PCR. Data are shown as mean ± SD for five mice in each recipient group. $*p < 0.05$; $**p < 0.005$. (**B**) FasL mRNA expressions in PBMCs of B6 and B6/*lpr* mice were analyzed by quantitative RT-PCR. Data are shown as mean ± SD for five mice in each recipient group. $*p < 0.05$. (**C**) FasL expression on the CD11b$^+$ macrophages in PBMCs was detected by flow cytometry. Results are representative of three independent experiments.

role in the Fas-mediated rapid death of normal T cells in B6/*lpr* mice.

*Functions of macrophages in B6/*lpr *mice*

To understand the functions of the peripheral macrophages in B6/*lpr* mice, macrophages from thioglycolate-elicited PECs were used for analyzing their interaction with normal T cells. When the expression level of FasL on PECs was analyzed, significantly increased expression of FasL on PECs from B6/*lpr* mice was detected compared with B6 mice (Fig. 4A). Next, we examined whether in vitro T cell death was induced by coculture with PECs from B6/*lpr* mice. The proportion of apoptotic T cells cocultured with B6/*lpr* PECs was significantly enhanced compared with that of normal T cells cocultured with B6 PECs (Fig. 4B). To determine whether B6/*lpr* PECs engulf dead T cells rapidly, CFSE-labeled normal T cells were cocultured with CD11b$^+$ PECs for 3 h, and CD11b$^+$CFSE$^+$ macrophages engulfing apoptotic T cells were analyzed. We detected a significant increase of CFSE$^+$ CD11b$^+$ macrophages in B6/*lpr* mice compared with B6 mice (Fig. 4C). In addition, we investigated the phagocytic activity of B6/*lpr* macrophages with FITC-labeled latex beads. The phagocytic activity of CD11b$^+$ PECs in B6/*lpr* mice was significantly increased compared with that in B6 mice (Fig. 4D). To rule out that the apoptotic cells attached to macrophages, we fixed the macrophages after phagocytosis assay and then treated them with 0.01% Triton X-100. Because there was no change in the proportion of CD11b$^+$FITC$^+$ macrophages between before and after Triton X treatment, the macrophages engulfed, but not bound to, the beads in this assay (Supplemental Fig. 2). These results suggest that enhanced FasL expression on the macrophages in B6/*lpr* mice triggers the rapid cell death of normal T cells in a Fas-deficient immune environment, and increased phagocytic activity of B6/*lpr* macrophages plays a key role in the clearance of dead T cells.

In vivo functions of Fas-deficient macrophages

To determine the in vivo functions of macrophages in B6/*lpr* mice, normal T cells from GFP-TG mice were i.p. injected into the recipient mice that had been injected with thioglycolate. At 6 h after T cell injection, PECs including injected T cells were analyzed. Consistent with the results obtained from the i.v. injection of normal T cells into B6/*lpr* mice, the T cells injected (i.p.) into B6/*lpr* mice were significantly decreased compared with those injected into B6 mice (Fig. 5A). The number of apoptotic cells showing Annexin V$^+$ of injected T cells in B6/*lpr* mice was significantly higher compared with that in B6 mice (Fig. 5B). The depletion of T cells in B6/*lpr* recipients was inhibited by i.p. injection of anti-FasL mAb (Fig. 5C). Furthermore, when normal

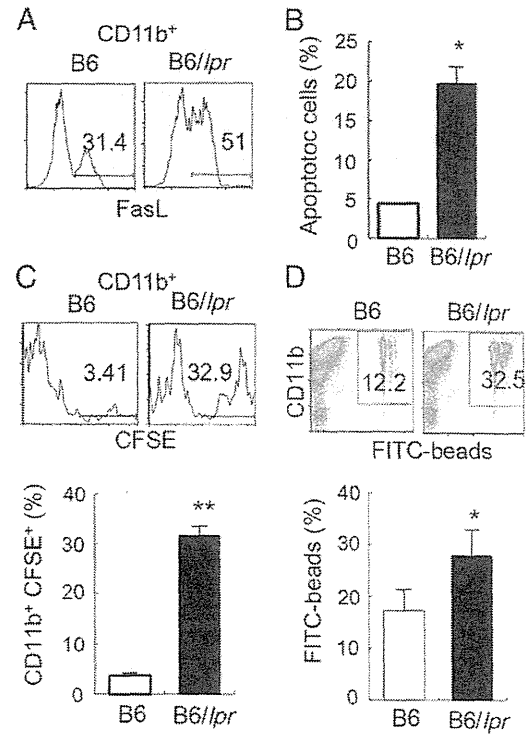

FIGURE 4. Enhanced FasL expression and phagocytotic activity of *lpr* macrophages in vitro. B6 and B6/*lpr* mice were i.p. injected with thioglycolate to obtain PECs. On day 4 after the injection, PECs were collected from peritoneal cavity. (**A**) FasL expression on CD11b$^+$ macrophages in PECs of B6 and B6/*lpr* mice was analyzed by flow cytometry. Data are representative of four independent experiments. (**B**) CFSE-labeled T cells from Thy1.1 B6 mice were cocultured with the CD11b$^+$ macrophages from PECs of B6 and B6/*lpr* mice. Annexin V$^+$ apoptotic T cells (percentage) are shown as mean ± SD for five mice in each group. $*p < 0.05$. (**C**) CFSE-labeled T cells from B6 mice were cocultured with the CD11b$^+$ macrophages from PECs of B6 and B6/*lpr* mice. Phagocytosis of CFSE$^+$ T cells by the CD11b$^+$ cells in PECs was evaluated by flow cytometry. Results are shown as mean ± SD for five mice in each group. $**p < 0.005$. (**D**) Phagocytic activity of CD11b$^+$ macrophages in PECs was evaluated by uptake of FITC-conjugated beads in vitro. Results are shown as mean ± SD for five mice in each group. $**p < 0.005$.

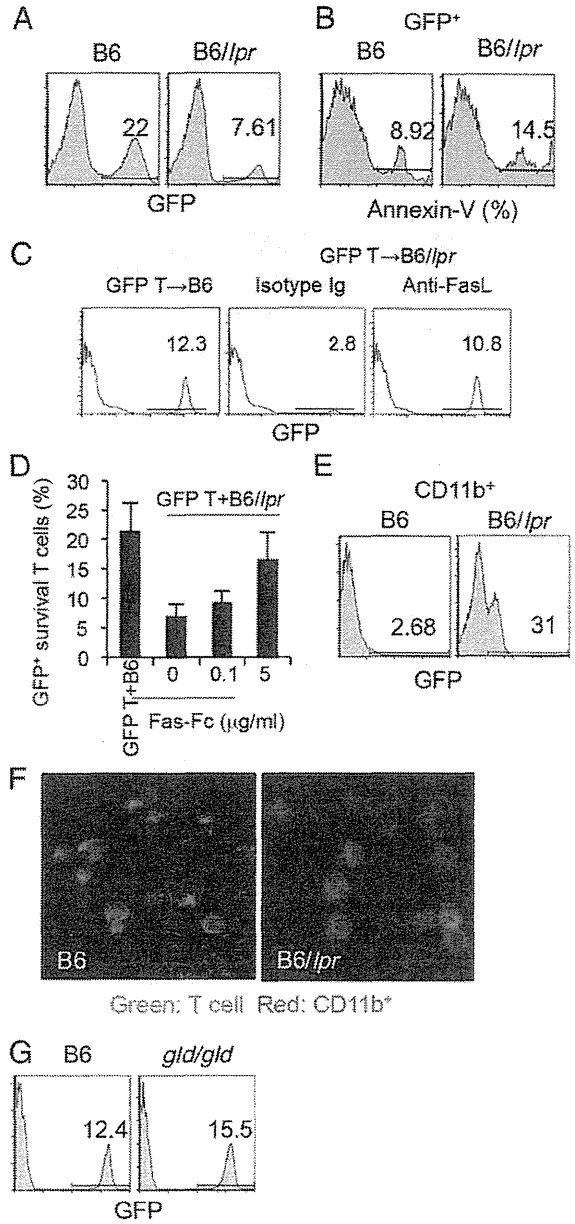

FIGURE 5. In vivo rapid death and phagocytosis of T cells by macrophages. (**A**) T cells (1×10^6) from GFP-TG mice were i.p. injected into the recipient mice treated with thioglycolate. GFP^+ T cells in PECs were detected by flow cytometry. Data are representative of four mice in each recipient group. (**B**) Annexin V^+ apoptotic cells (percentage) of GFP^+ T cells in PECs were detected by flow cytometry. Data are representative of four mice in each recipient group. (**C**) GFP T cells (1×10^6) were i.p. injected into thioglycolate-treated B6/*lpr* recipients together with anti-Fas mAb or isotype control Ig. (**D**) GFP T cells (5×10^4) were cocultured with B6/*lpr* PECs (2×10^5) fro 24 h in vitro in the presence of Fas-Fc fusion protein (0, 0.1, and 5 μg/ml). GFP^+ survival cells are shown as mean ± SD for triplicates. (**E**) Phagocytosis of GFP^+ T cells by the $CD11b^+$ macrophages in PECs was evaluated by flow cytometry. Data are representative of four mice in each recipient group. (**F**) GFP^+ T cells (green) and $CD11b^+$ macrophages (red) in PECs were detected by confocal microscopy. Original magnification ×630. Data are representative of four three independent experiments. (**G**) T cells from GFP-TG mice were i.p. injected into B6 and B6/*gld* mice treated with thioglycolate. GFP^+ T cells in PECs were detected by flow cytometry. Data are representative of four mice in each recipient group.

GFP-T cells were i.p. transferred into B6/*lpr* mice together with Fas-Fc fusion protein (0.1 and 5 μg/ml), survival T cells were significantly increased in comparison with those of the recipients without Fas-Fc (Fig. 5D). In addition, the phagocytic activity of $CD11b^+$ PECs in B6/*lpr* was significantly enhanced compared with that in B6/mice (Fig. 5E). Furthermore, microscopic analysis showed fewer normal T cells (GFP^+) in B6/*lpr* mice compared with B6 mice: moreover, it revealed phagocytic fragments of GFP^+ T cells within the macrophages in B6/*lpr* mice, although the fragments within the macrophages in B6 mice were undetectable (Fig. 5F). In contrast, when normal T cells from GFP-TG mice were i.p. injected into B6 and B6/*gld* mice, which are deficient in FasL expression, T cell diminishment was not observed (Fig. 5G). In contrast, we have performed the experiment using purified B cells. Because deletion of normal B cells in *lpr* recipients was not observed (Supplemental Fig. 3), T cell apoptosis may be closely associated with phagocytosis of *lpr* macrophages. Our findings reveal that Fas-deficient macrophages can induce rapid apoptosis through upregulated FasL and that Fas-deficient macrophages rapidly engulf apoptotic T cells.

Enhanced activation of Fas-deficient macrophages through NF-κB

NF-κB signaling plays a crucial role in the activation of macrophages (22, 23). Phosphorylation of IκBα, an endogenous inhibitory molecule of NF-κB activation by the interaction with NF-κB subunits, in $CD11b^+$PECs from B6/*lpr* mice was much higher than that in $CD11b^+$ PECs from B6 mice (Fig. 6A). Moreover, nuclear transport of NF-κB subunits such as p50 and p65 in $CD11b^+$ PECs from B6/*lpr* mice was significantly enhanced compared with that in $CD11b^+$ PECs from B6 mice (Fig. 6A). In addition, the transcriptional activity of NF-κB in the nuclear protein of the $CD11b^+$ PECs from B6/*lpr* mice was significantly increased compared with that from B6 mice (Fig. 6B). In immune cells, including macrophages, there are several genes regulated by NF-κB such as TNF-α, IL-6, IL-1β, and FasL in immune cells including macrophage (24–27). The mRNA expression of TNF-α, IL-6, and IL-1β in $CD11b^+$ PECs from B6/*lpr* mice was not increased compared with that from B6 mice (Fig. 6C). In contrast, the FasL mRNA level in the $CD11b^+$ PECs from B6/*lpr* mice was significantly higher than that from B6 mice (Fig. 6D). When FasL mRNA of the $CD11b^+$ PECs from $NF\text{-}\kappa B_1$ gene knockout mice bearing a *fas* gene mutant ($NF\text{-}\kappa B_1^{-/-}$/*lpr*) was analyzed, the expression level was similar to that of B6 mice (Fig. 6D). Furthermore, the diminishment of normal T cells in $NF\text{-}\kappa B_1^{-/-}$/*lpr* mice was not observed (Fig. 6E, 6F). These results suggest that FasL overexpression through NF-κB activation of macrophages is important for rapid T cell death in a Fas-deficient immune system.

Alteration of Fas expression on normal T cells in a Fas-deficient immune system

Fas expression is regulated by several factors or signaling pathways (28–31). One potent factor that induces Fas expression is IFN-γ (28). When the serum level of IFN-γ was analyzed by ELISA, we found that the concentration of the sera in B6/*lpr* mice was significantly higher compared with that in B6 mice (Fig. 7A). To determine the source of the high level of IFN-γ, subsets of peripheral immune cells including $CD4^+$ T cells, $CD8^+$ T cells, $CD11b^+$ macrophages, $CD11c^+$ dendritic cells, and $B220^+$ B cells in PBMCs were purified, and IFN-γ mRNA was analyzed by quantitative RT-PCR. The mRNA levels in $CD4^+$, $CD8^+$ T, and $B220^+$ B cells from B6/*lpr* mice increased significantly compared with those in B6 mice (Fig. 7B). When the T cells from normal mice or $IFN\gamma R^{-/-}$ mice were labeled with CFSE and were i.v. injected into B6/*lpr* mice, Fas expression on T cells in $IFN\gamma R^{-/-}$ mice was not enhanced, although the expression on T cells from B6 mice was considerably increased in Fas-deficient recipients

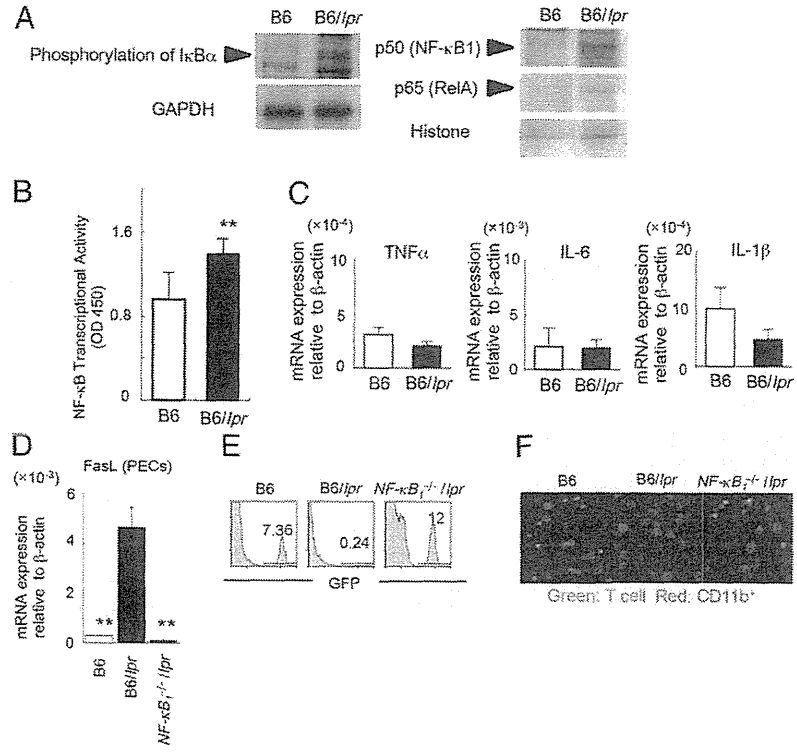

FIGURE 6. Control of FasL expression on *lpr* macrophages by NF-κB activation. (**A**) Phosphorylation of IκBα and nuclear translocation of the NF-κB subunits of CD11b$^+$ macrophages from thioglycolate-induced PECs were analyzed by Western blotting. GAPDH and histones were used as housekeeping proteins. Data are representative of three independent experiments. (**B**) Transcriptional activity of NF-κB in B6 and B6/*lpr* macrophages was detected. Results are shown as mean ± SD for five mice in each group. $^{**}p < 0.005$. (**C**) The mRNA expression of NF-κB–target genes was analyzed by quantitative RT-PCR. Data are shown as mean ± SD for five mice in each group. (**D**) FasL mRNA expression in the CD11b$^+$ macrophages from thioglycolate-induced PECs in B6, B6/*lpr*, and *NF-κB1*$^{-/-}$/*lpr* mice was analyzed by quantitative RT-PCR. Data are shown as mean ± SD for five mice in each group. $^{**}p < 0.005$. (**E**) T cells from GFP-TG mice were i.p. injected into B6, B6/*lpr*, and *NF-κB1*$^{-/-}$/*lpr* mice pretreated with thioglycolate. GFP$^+$ T cells in PECs were detected by flow cytometry. Data are representative of five mice in each group. (**F**) GFP$^+$ T cells (green) and CD11b$^+$ macrophages (red) in PECs were detected by confocal microscopy. Original magnification ×630. Photos are representative of four independent experiments.

(Fig. 7C). Fas expression on T cells was enhanced by recombinant IFN-γ in a dose-dependent manner (Supplemental Fig. 4). In addition, when T cells from *IFNγR*$^{-/-}$ mice were i.v. injected into B6/*lpr* mice, T cell diminishment, which had been observed in the Fas-deficient recipients, was not detectable (Fig. 7D). Moreover, when T cells from *IFNγR*$^{-/-}$ mice were cocultured with *lpr* PECs, survival T cells of *IFNγR*$^{-/-}$ mice were significantly increased compared with those of wild-type mice (Fig. 7E). By the

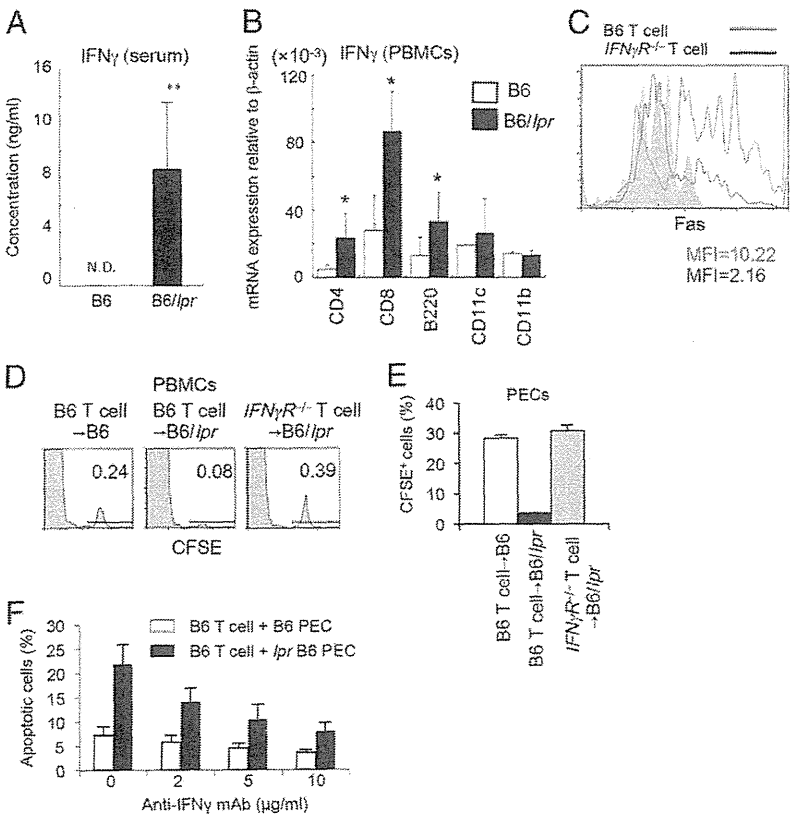

FIGURE 7. Regulation of Fas expression on donor T cells by IFN-γ in *lpr* mice. (**A**) Concentration of IFN-γ in the sera of B6 and B6/*lpr* mice was measured by ELISA. Results are shown as mean ± SD for six mice in each group. $^{**}p < 0.005$. (**B**) IFN-γ mRNA expressions in the subsets of spleen cells from B6 and B6/*lpr* mice were analyzed by quantitative RT-PCR. Results are shown as mean ± SD for five mice in each group. $^{*}p < 0.05$. (**C**) CFSE-labeled T cells from B6 and *IFNγR*$^{-/-}$ mice were i.v. injected into B6/*lpr* mice. Fas expression on the donor T cells in PBMCs of recipients was analyzed by flow cytometry. Data are representative of five mice in each group. Gray shadow shows isotype negative control. (**D**) CFSE-labeled T cells from B6 and *IFNγR*$^{-/-}$ mice were i.v. injected into B6 or B6/*lpr* mice and were detected by flow cytometry. Data are representative of four mice in each group. (**E**) CFSE-labeled T cells from B6 and *IFNγR*$^{-/-}$ mice were i.p. injected into thioglicolate-treated B6 or B6/*lpr* mice. CFSE$^+$ T cells in PECs were analyzed by flow cytometry. Results are shown as mean ± SD for four mice in each group. (**F**) T cells (2×10^4) from B6 mice were cocultured for 8 h with B6 or B6/*lpr* PECs (1×10^5) in the presence of anti–IFN-γ mAb (0, 2, 5, and 10 μg/ml). Apoptotic T cells were evaluated by flow cytometric analysis of expression of Annexin V. Results are shown as mean ± SD for triplicates in each group.

pretreatment of anti–IFN-γ mAb, apoptosis of normal activated T cell interacted with *lpr* PECs was inhibited in the dose-dependent manner (Fig. 7F). These findings suggest that the high level of IFN-γ in B6/*lpr* mice enhances Fas expression on injected normal T cells and that immune cells in B6/*lpr* mice highly expressing FasL induce Fas-mediated and rapid apoptosis of T cells.

Discussion

In this study, we confirmed that normal T cells failed to survive in a Fas-deficient immune condition using the transfer experiments. In addition, the homeostatic proliferation of T cells in lymphopenic recipients of *lpr* mice and Ag-specific T cell response in *lpr* mice were not observed. These findings are consistent with the results in the previous reports regarding the failure of normal lymphocyte survival in *lpr* hosts (17, 18). The phenomenon was thought to occur because of the induction of T cell apoptosis in *lpr* recipients because the transferred T cells did not migrate in any specific organs other than lymphoid tissues and the liver.

Because the diminishment of normal T cells was observed in PBMCs in 30 min immediately after the transfer, rapid death of transferred T cells may have occurred in *lpr* recipients. However, T cell diminishment in *lpr* donor mice was undetectable. Thus, the rapid T cell death occurred by the presence or absence of the Fas molecule on these cells.

Although enhanced FasL expression on immune cells in *lpr* mice has been described previously (18, 20), it was unclear as to which subset of immune cells in *lpr* mice overexpressed FasL molecule. In this study, mRNA expression of FasL of all subsets in the spleen and PBMCs of *lpr* mice was significantly higher than that of control mice. In particular, FasL mRNA expression in $CD11b^+$ macrophages in *lpr* mice was significantly increased compared with that in control mice. In addition, when thioglycolate-elicited PECs, including a number of macrophages, were used to analyze the interaction with T cell in vivo and in vitro, enhanced rapid death and clearance of T cells by *lpr* macrophages was observed. Furthermore, phagocytic activity of *lpr* macrophages was considerably enhanced compared with control macrophages. These results suggest that *lpr* macrophages can phagocyte apoptotic T cells promptly as well as induce the rapid T cell death in the periphery. The *lpr* macrophages with enhanced expression of FasL may induce rapid death of T cells and promptly engulf the apoptotic cells by FasL-independent phagocytosis. There may be unknown cellular mechanism like "Eat me signal."

FasL, a type II transmembrane protein belonging to the TNF superfamily, is a well-characterized apoptosis initiating protein (32–34). Some transcription factors have been shown to regulate FasL gene expression, including specificity protein-1, IFN regulatory factor-1, NF in activated T cells and NF-κB (35–37). NF-κB plays key roles in differentiation and activation of macrophages (22, 38). Our results suggest that the direct contribution of macrophages to the induction of rapid death of T cells is very important for effective phagocytosis of apoptotic T cells. Furthermore, our results imply that the induction of expression of FasL in macrophages by NF-κB is negatively controlled by Fas signaling. This is related to our previous report that Fas signaling controls RANKL signaling following NF-κB activation in dendritic cells (39). Fas signaling may play important roles in NF-κB activation in relation to cell activation, survival, and growth in addition to apoptosis.

As to the relationship between FasL expression and phagocytosis in macrophages, it was reported that enhanced expression of FasL on Kupffer cells is associated with phagocytosis of apoptotic T cells in human liver allografts (40). Although further experiments will be needed to confirm the cellular mechanism, FasL-enhanced macrophages may engulf apoptotic cells effectively.

It is widely established that Fas expression on peripheral T cells plays a key role in AICD to maintain peripheral immune system (2, 3, 5). Fas expression on T cells increases by TCR signaling (41). In addition, some cytokines such as IL-2 and/or IFN-γ trigger the enhancement of Fas expression on T cells (42). Our results imply that an extremely high concentration of IFN-γ in the serum of *lpr* mice acts on the induction of Fas expression on the transferred T cells directly. When T cells from IFN-γR knockout mice were transferred into *lpr* mice, the rapid death and diminishment of T cells was not observed. These results strongly suggest that Fas expression on peripheral T cells is controlled through the IFN-γ/IFN-γR.

With regard to the control of the Fas expression of cells other than the T cell, it was reported that TNF-α can control the expression of fibroblasts in addition to IFN-γ (30). Although we found a high concentration of IFN-γ in the serum from *lpr* mice, the level of TNF-α concentration in the serum from *lpr* mice was similar to that from control mice (data not shown). In this study, when naive T cells from normal mice were transferred, they were not activated and slightly expressed the Fas molecule on the cell surface. Because of the exposure to the high concentration of IFN-γ in *lpr* mice, Fas expression on T cells rapidly increased. The immune cells highly expressing FasL including macrophages of *lpr* mice may induce the rapid apoptosis of T cells, and the macrophages in the peripheral immune system may rapidly phagocytize the apoptotic T cells.

In contrast, many reports indicate that B cells are maintained by Fas and Bim-dependent apoptosis to protect autoimmunity (43–45). In our experiment, $CD19^+$ B cells failed to undergo apoptosis in Fas-deficient host, although FasL expression on immune cells was enhanced. This finding implies that rapid T cell death may be triggered by cell–cell contact between normal T cells and Fas-deficient macrophages through the interaction with cell surface molecules such as MHC class II, costimulatory molecules, or TCR, although its precise mechanism has been still clarified.

Our results suggest that Fas signaling contributes to nonapoptotic functions such as the phagocytic activity of macrophages. Fas promotes the differentiation, proliferation, and maturation in several cells (1, 2, 46). Fas-associated death domain–mediated activation of caspase 8 is essential for the process of apoptosis of various cells (12, 47). In addition, it was reported that Rho GTPase Rac1 sensitizes T cells to Fas-induced apoptosis correlated with Rac-mediated cytoskeletal reorganization, dephosphorylation of the ezrin/radixin/moesin family of cytoskeletal linker proteins, and the translocation of Fas to lipid raft microdomain (48). However, the molecular mechanism for controlling the phagocytic activity of macrophages through Fas signaling has yet to be elucidated.

Although it has been reported that normal immune cells failed to survive in *lpr* recipients, the precise mechanism for its phenomenon remained unclear. In this study, we found that abnormal macrophages in *lpr* mice play critical roles in the disorder of the peripheral immune system. Our findings are thought to be important for therapeutic strategies for immune disorders such as ALPS or the other autoimmune diseases related to the abnormal expression of Fas on immune cells. In addition, this study suggests that Fas expression on macrophages contributes to the survival of T cells in the peripheral immune system. Taken together, this study strongly suggests that Fas-expressing macrophages play a pivotal role in maintaining T cell homeostasis in addition to AICD in the periphery.

Acknowledgments

We thank S. Katada, A. Katayama, and N. Kino for technical assistance.

Disclosures

The authors have no financial conflicts of interest.

References

1. Nagata, S. 1997. Apoptosis by death factor. *Cell* 88: 355–365.
2. Krammer, P. H. 2000. CD95's deadly mission in the immune system. *Nature* 407: 789–795.
3. Strasser, A., P. J. Jost, and S. Nagata. 2009. The many roles of FAS receptor signaling in the immune system. *Immunity* 30: 180–192.
4. Alderson, M. R., T. W. Tough, T. Davis-Smith, S. Braddy, B. Falk, K. A. Schooley, R. G. Goodwin, C. A. Smith, F. Ramsdell, and D. H. Lynch. 1995. Fas ligand mediates activation-induced cell death in human T lymphocytes. *J. Exp. Med.* 181: 71–77.
5. Maher, S., D. Toomey, C. Condron, and D. Bouchier-Hayes. 2002. Activation-induced cell death: the controversial role of Fas and Fas ligand in immune privilege and tumour counterattack. *Immunol. Cell Biol.* 80: 131–137.
6. Zhang, J., X. Xu, and Y. Liu. 2004. Activation-induced cell death in T cells and autoimmunity. *Cell. Mol. Immunol.* 1: 186–192.
7. Shultz, L. D., and C. L. Sidman. 1987. Genetically determined murine models of immunodeficiency. *Annu. Rev. Immunol.* 5: 367–403.
8. Jabs, D. A., and R. A. Prendergast. 1988. Murine models of Sjögren's syndrome: immunohistologic analysis of different strains. *Invest. Ophthalmol. Vis. Sci.* 29: 1437–1443.
9. Cohen, P. L., and R. A. Eisenberg. 1991. Lpr and gld: single gene models of systemic autoimmunity and lymphoproliferative disease. *Annu. Rev. Immunol.* 9: 243–269.
10. Kotzin, B. L. 1996. Systemic lupus erythematosus. *Cell* 85: 303–306.
11. Singer, P. A., and A. N. Theofilopoulos. 1990. Novel origin of lpr and gld cells and possible implications in autoimmunity. *J. Autoimmun.* 3: 123–135.
12. Boldin, M. P., E. E. Varfolomeev, Z. Pancer, I. L. Mett, J. H. Camonis, and D. Wallach. 1995. A novel protein that interacts with the death domain of Fas/APO1 contains a sequence motif related to the death domain. *J. Biol. Chem.* 270: 7795–7798.
13. Scaffidi, C., S. Fulda, A. Srinivasan, C. Friesen, F. Li, K. J. Tomaselli, K. M. Debatin, P. H. Krammer, and M. E. Peter. 1998. Two CD95 (APO-1/Fas) signaling pathways. *EMBO J.* 17: 1675–1687.
14. Curtin, J. F., and T. G. Cotter. 2003. Live and let die: regulatory mechanisms in Fas-mediated apoptosis. *Cell. Signal.* 15: 983–992.
15. Hughes, P. D., G. T. Belz, K. A. Fortner, R. C. Budd, A. Strasser, and P. Boullet. 2008. Apoptosis receptors Fas and Bim coorerate I shutdown of chronic immune receptors and prevention of autoimmunity. *Immunity* 28: 197–205.
16. Green, D. R., and M. Schuler. 2000. T cell development: some cells get all the breaks. *Nat. Immunol.* 1: 15–17.
17. Ettinger, R., J. K. Wang, P. Bossu, K. Papas, C. L. Sidman, A. K. Abbas, and A. Marshak-Rothstein. 1994. Functional distinctions between MRL-lpr and MRL-gld lymphocytes: normal cells reverse the gld but not lpr immunoregulatory defect. *J. Immunol.* 152: 1557–1568.
18. Wei, Y., K. Chen, G. C. Sharp, and H. Braley-Mullen. 2004. Fas ligand is required for resolution of granulomatous experimental autoimmune thyroiditis. *J. Immunol.* 173: 7615–7621.
19. Theofilopoulos, A. N., R. S. Balderas, Y. Gozes, M. T. Aguado, L. M. Hang, P. R. Morrow, and F. J. Dixon. 1985. Association of lpr gene with graft-vs.-host disease-like syndrome. *J. Exp. Med.* 162: 1–18.
20. Chu, J. L., P. Ramos, A. Rosendorff, J. Nikolić-Zugić, E. Lacy, A. Matsuzawa, and K. B. Elkon. 1995. Massive upregulation of the Fas ligand in lpr and gld mice: implications for Fas regulation and the graft-versus-host disease-like wasting syndrome. *J. Exp. Med.* 181: 393–398.
21. Allison, J., and A. Strasser. 1998. Mechanisms of β cell death in diabetes: a minor role for CD95. *Proc. Natl. Acad. Sci. USA* 95: 13818–13822.
22. Hawiger, J. 2001. Innate immunity and inflammation: a transcriptional paradigm. *Immunol. Res.* 23: 99–109.
23. Spehlmann, M. E., and L. Eckmann. 2009. Nuclear factor-κB in intestinal protection and destruction. *Curr. Opin. Gastroenterol.* 25: 92–99.
24. Dunn, S. M., L. S. Coles, R. K. Lang, S. Gerondakis, M. A. Vadas, and M. F. Shannon. 1994. Requirement for nuclear factor (NF)-κB p65 and NF-interleukin-6 binding elements in the tumor necrosis factor response region of the granulocyte colony-stimulating factor promoter. *Blood* 83: 2469–2479.
25. Baer, M., A. Dillner, R. C. Schwartz, C. Sedon, S. Nedospasov, and P. F. Johnson. 1998. Tumor necrosis factor α transcription in macrophages is attenuated by an autocrine factor that preferentially induces NF-κB p50. *Mol. Cell. Biol.* 18: 5678–5689.
26. Mercurio, F., and A. M. Manning. 1999. Multiple signals converging on NF-κB. *Curr. Opin. Cell Biol.* 11: 226–232.
27. Torgler, R., S. Jakob, E. Ontsouka, U. Nachbur, C. Mueller, D. R. Green, and T. Brunner. 2004. Regulation of activation-induced Fas (CD95/Apo-1) ligand expression in T cells by the cyclin B1/Cdk1 complex. *J. Biol. Chem.* 279: 37334–37342.
28. Nagafuji, K., T. Shibuya, M. Harada, S. Mizuno, K. Takenaka, T. Miyamoto, T. Okamura, H. Gondo, and Y. Niho. 1995. Functional expression of Fas antigen (CD95) on hematopoietic progenitor cells. *Blood* 86: 883–889.
29. De Maria, R., and R. Testi. 1998. Fas-FasL interactions: a common pathogenetic mechanism in organ-specific autoimmunity. *Immunol. Today* 19: 121–125.
30. Frankel, S. K., G. P. Cosgrove, S. I. Cha, C. D. Cool, M. W. Wynes, B. L. Edelman, K. K. Brown, and D. W. Riches. 2006. TNF-α sensitizes normal and fibrotic human lung fibroblasts to Fas-induced apoptosis. *Am. J. Respir. Cell Mol. Biol.* 34: 293–304.
31. Wynes, M. W., B. L. Edelman, A. G. Kostyk, M. G. Edwards, C. Coldren, S. D. Groshong, G. P. Cosgrove, E. F. Redente, A. Bamberg, K. K. Brown, et al. 2011. Increased cell surface Fas expression is necessary and sufficient to sensitize lung fibroblasts to Fas ligation-induced apoptosis: implications for fibroblast accumulation in idiopathic pulmonary fibrosis. *J. Immunol.* 187: 527–537.
32. Ju, S. T., D. J. Panka, H. Cui, R. Ettinger, M. el-Khatib, D. H. Sherr, B. Z. Stanger, and A. Marshak-Rothstein. 1995. Fas(CD95)/FasL interactions required for programmed cell death after T-cell activation. *Nature* 373: 444–448.
33. Janssen, O., J. Qian, A. Linkermann, and D. Kabelitz. 2003. CD95 ligand—death factor and costimulatory molecule? *Cell Death Differ.* 10: 1215–1225.
34. Lettau, M., M. Paulsen, H. Schmidt, and O. Janssen. 2011. Insights into the molecular regulation of FasL (CD178) biology. *Eur. J. Cell Biol.* 90: 456–466.
35. Chow, W. A., J. J. Fang, and J. K. Yee. 2000. The IFN regulatory factor family participates in regulation of Fas ligand gene expression in T cells. *J. Immunol.* 164: 3512–3518.
36. Jayanthi, S., X. Deng, B. Ladenheim, M. T. McCoy, A. Cluster, N. S. Cai, and J. L. Cadet. 2005. Calcineurin/NFAT-induced up-regulation of the Fas ligand/Fas death pathway is involved in methamphetamine-induced neuronal apoptosis. *Proc. Natl. Acad. Sci. USA* 102: 868–873.
37. Yao, P. L., Y. C. Lin, P. Sawhney, and J. H. Richburg. 2007. Transcriptional regulation of FasL expression and participation of sTNF-α in response to sertoli cell injury. *J. Biol. Chem.* 282: 5420–5431.
38. Lawrence, T., and G. Natoli. 2011. Transcriptional regulation of macrophage polarization: enabling diversity with identity. *Nat. Rev. Immunol.* 11: 750–761.
39. Izawa, T., N. Ishimaru, K. Moriyama, M. Kohashi, R. Arakaki, and Y. Hayashi. 2007. Crosstalk between RANKL and Fas signaling in dendritic cells controls immune tolerance. *Blood* 110: 242–250.
40. Miyagawa-Hayashino, A., T. Tsuruyama, H. Egawa, H. Haga, H. Sakashita, T. Okuno, S. Toyokuni, K. Tamaki, H. Yamabe, T. Manabe, and S. Uemoto. 2007. FasL expression I hepatic antigen-presenting cells and phagocytosis of apoptotic T cells by FasL$^+$ kupffer cells are indicators of rejection activity in human liver allografts. *Am. J. Pathol.* 177: 1499–1508.
41. Marrack, P., and J. Kappler. 2004. Control of T cell viability. *Annu. Rev. Immunol.* 22: 765–787.
42. Carter, L. L., X. Zhang, C. Dubey, P. Rogers, L. Tsui, and S. L. Swain. 1998. Regulation of T cell subsets from naive to memory. *J. Immunother.* 21: 181–187.
43. Hutcheson, J., J. C. Scatizzi, A. M. Siddiqui, G. K. Haines, III, T. Wu, Q. Z. Li, L. S. Davis, C. Mohan, and H. Perlman. 2008. Combined deficiency of proapoptotic regulators Bim and Fas results in the early onset of systemic autoimmunity. *Immunity* 28: 206–217.
44. Bouillet, P., D. Metcalf, D. C. Huang, D. M. Tarlinton, T. W. Kay, F. Köntgen, J. M. Adams, and A. Strasser. 1999. Proapoptotic Bcl-2 relative Bim required for certain apoptotic responses, leukocyte homeostasis, and to preclude autoimmunity. *Science* 286: 1735–1738.
45. Enders, A., P. Bouillet, H. Puthalakath, Y. Xu, D. M. Tarlinton, and A. Strasser. 2003. Loss of the pro-apoptotic BH3-only Bcl-2 family member Bim inhibits BCR stimulation-induced apoptosis and deletion of autoreactive B cells. *J. Exp. Med.* 198: 1119–1126.
46. Peter, M. E., R. C. Budd, J. Desbarats, S. M. Hedrick, A. O. Hueber, M. K. Newell, L. B. Owen, R. M. Pope, J. Tschopp, H. Wajant, et al. 2007. The CD95 receptor: apoptosis revisited. *Cell* 129: 447–450.
47. Muzio, M., A. M. Chinnaiyan, F. C. Kischkel, K. O'Rourke, A. Shevchenko, J. Ni, C. Scaffidi, J. D. Bretz, M. Zhang, R. Gentz, et al. 1996. FLICE, a novel FADD-homologous ICE/CED-3-like protease, is recruited to the CD95 (Fas/APO-1) death—inducing signaling complex. *Cell* 85: 817–827.
48. Ramaswamy, M., C. Dumont, A. C. Cruz, J. R. Muppidi, T. S. Gomez, D. D. Billadeau, V. L. Tybulewicz, and R. M. Siegel. 2007. Cutting edge: Rac GTPases sensitize activated T cells to die via Fas. *J. Immunol.* 179: 6384–6388.

18

Irreversible Effects of Diethylstilbestrol on Reproductive Organs and a Current Approach for Epigenetic Effects of Endocrine Disrupting Chemicals

Shinichi Miyagawa,[1] Ryohei Yatsu,[1] Tamotsu Sudo,[2] Katsuhide Igarashi,[3] Jun Kanno,[3] and Taisen Iguchi[1]

[1] *Okazaki Institute for Integrative Bioscience, National Institute for Basic Biology, National Institutes of Natural Sciences, and Department of Basic Biology, The Graduate University for Advanced Studies, Okazaki, Aichi, Japan*

[2] *Section of Translational Research and Development of Gynecological Oncology, Hyogo Cancer Center, Akashi, Hyogo, Japan*

[3] *Division of Cellular and Molecular Toxicology, National Institute of Health Sciences, Setagaya-ku, Tokyo, Japan*

18.1 Introduction

Chemicals released into the environment potentially disrupt the endocrine system in wild animals and humans. For years, possible endocrine disruption in animals exposed to such chemicals (endocrine disrupting chemicals; EDCs), and the implication for wildlife has been investigated. The embryonic developmental period, in particular, has been extensively discussed among scholars, due to its marked higher fragility and sensitivity to foreign influences. Considering both the immediate and latent disruption of internal physiology from embryonic contamination, as well as the enormous amount of health damage associated with it, the clarification of the molecular basis of functional effects of EDCs and endogenous estrogens on developing organisms is essential and should be prioritized.

Toxicology and Epigenetics, First Edition. Edited by Saura C. Sahu.

The subdiscipline of toxicogenomics, combining the fields of genomics and toxicology, has been utilized to evaluate the risks of chemical exposures to humans and animals, using a wide assortment of techniques. DNA microarrays, for instance, are commonly used to evaluate such risks by providing a high throughput diagnostic of genetic conditions, and have been successfully applied for genome-wide analysis of gene expression stimulated by hormones and/or EDCs. To briefly illustrate this field and its focus, we present our past murine research as an example.

Using cDNA microarrays, we have been able to identify estrogen/EDCs-responsive genes in the female mouse reproductive tracts (Watanabe *et al.*, 2003a,b, 2002). Our results indicated a large number of genes affected by estrogens, and expressions of most of the genes were induced in a dose-dependent manner. Moreover, their expression was not altered in ERα knockout mice (ER, estrogen receptor), thus confirming the dependency of these genes on ERα in female mouse reproductive tracts. On the other hand, characteristic gene expression patterns were also observed for each experimental EDC exposures, and these patterns were distinct from that of 17β-estradiol (E2), suggesting separate and specific mechanisms of action for EDCs. Thus, knowledge of the patterns in the expression of estrogen/EDCs-responsive genes is essential for understanding the action mechanism of estrogenic chemicals, and the profiling of transcripts can prove helpful in understanding modes of action of EDCs and toxicants.

To summarize, EDCs can deleteriously modify gene expression and disrupt normal development on developing animals, and the subsequent malformation of phenotypic characteristic does not become apparent until much later in life. EDCs thus differ from classical teratogens and therefore, the molecular approach is particularly important for evaluating such long-term effects of EDCs on developing animals. In this chapter, an irreversible effect of diethylstilbestrol (DES) on reproductive organs and the current approach for investigating epigenetic effects of EDCs are discussed.

18.2 Adverse effects of perinatally-exposed DES on the mouse vagina

To understand the molecular basis of EDCs and endogenous estrogen on developing organisms, we need to first explore the linkages between the genes responsive to EDCs and the adverse effects induced by these chemicals. Only by first establishing the basic elements that govern the internal endocrine system and the corresponding genetic pathways during development, can one accurately deduce the specifics of molecular interaction with EDCs, and to a greater extent, provide a genetic explanation for the abnormal phenotypic outcome. To address such a criterion, the perinatal mouse model has often been used to demonstrate the long-term effects of estrogens and EDCs in female reproductive organs.

One of the best-studied cases using the said model is DES, a synthetic estrogen. From the 1940s, DES was routinely prescribed to pregnant women for the prevention of miscarriages. To date, it is well-known that in utero exposure to DES induces vaginal clear-cell adenocarcinoma and various malformations in the reproductive organs in young women (Herbst, Ulfelder, and Poskanzer, 1971). More than 95% of females exposed to DES in utero had some abnormalities, and the risk of cancer after the age of 50 increased threefold in their reproductive organs (Newbold, 2004; Palmer *et al.*, 2006). Like humans, perinatal female mice exposed to DES develop estrogen-independent persistent cell proliferation, stratification, and cornification of the vaginal epithelium, resulting in hyperplastic lesions and vaginal cancer later in life (McLachlan, Newbold, and Bullock, 1980; Takasugi, Bern, and Deome, 1962). Based on the gene expression analysis, we found an estrogen-independent expression of ~~EGF-like (epidermal growth factor)~~ growth factors and activation of the following phosphorylation cascades involving erbBs receptors, MAPK (mitogen-activated protein kinase) and Akt signalings in neonatally DES-exposed mouse vagina (Miyagawa *et al.*, 2004a,b). Such growth factor signaling is tightly regulated by endogenous estrogen in the normal mice. The activation of growth factor pathway in turn induces phosphorylation of the ~~AF-1 (activation function)~~ domain of ERα even in the absence of endogenous estrogen by removing the ovary. It has been shown that phosphorylation of ERα induces transcription activity in a ligand-independent manner through AF-1 (Kato *et al.*, 1995).

Thus, persistent growth factor expression could be the most likely mechanism for formation of cancerous lesions later in life.

How can experience of DES exposure exclusively during the neonatal period result in persistent gene misexpression in adulthood? Although the precise mechanisms have not been established explaining how such an activation loop with persistent gene misexpression is elicited, accumulating evidence suggests that DNA methylation might have an important role in this process. DNA methylation is a key epigenetic modification, a process that influences the phenotypic outcome of a gene without genetic changes of the underlying DNA sequence.

Modification of methylation at promoter region of the gene is now considered to be a common mechanism for epigenetic inheritance, as evidenced from epigenetic cancer studies (Jones and Baylin, 2002). Prenatal DES exposure alters methylation patterns in the promoter of some estrogen-responsive genes, including the demethylation of the c-fos and lactoferrin genes in the Müllerian duct (Li *et al.*, 1997, 2003). C-fos is a growth promoter that can predispose cells to becoming tumors. Hypomethylation of the nucleosomal binding protein 1 (Nsbp1) gene and its subsequent elevated expression is also reported after neonatal exposure to either DES or genistein (Tang *et al.*, 2008). Neonatal estrogen- or bisphenol A-exposure in rats induces hypomethylation of phosphodiesterase a type 4 variant 4 (PDE4D4) gene, resulting in elevated expression of this gene in the prostate (Ho *et al.*, 2006). PDE4D4 is a crucial regulator for cAMP degradation and suggests a correlation between its expression and development of prostatic intraepithelial neoplasia. Thus, epigenetic changes could lead to altered gene expression and result in alteration of tissue differentiation and formation, which could then lead to an increased susceptibility to disease and dysfunction later in life.

DES can also act as a teratogen in the developing fetuses and neonates. For example, misregulation of Wnt and Hox genes in the Müllerian duct by DES causes the formation of abnormal boundary between the oviduct, uterus, and vagina (Block *et al.*, 2000; Ma *et al.*, 1998; Miller, Degenhardt, and Sassoon, 1998). It has been shown that the frequency of DNA methylation in the Hoxa10 intron is higher in prenatally DES-exposed mice when compared with controls (Bromer *et al.*, 2009). Hoxa10 is associated with a variety of aspects of cellular physiology and women's health. Although altered methylation by DES exposure in humans has not been reported, downregulation of Hoxa10 expression and aberrant methylation of the Hoxa10 gene is associated with endometrial carcinoma and endometriosis in humans (Taylor *et al.*, 1998; Wu *et al.*, 2005; Yoshida *et al.*, 2006).

Environmental agents can thus significantly alter gene expression, and therefore result in an unexpected phenotype by changing the DNA methylation pattern. However, the cellular process underlying this very phenomenon remains unknown. Unraveling the epigenetic status would, therefore, be critical for understanding the molecular basis of action of EDCs and toxicological effects of estrogens in developing animals. We thus provide an overview of our current approach for understanding molecular effects of EDCs using toxicogenomic approaches.

18.3 MeDIP-ChIP

In mammals, DNA methylation primarily occurs at the fifth position of the cytosine residue in CpG dinucleotides. The methylated DNA immunoprecipitation (MeDIP) procedure is based on the enrichment of methylated DNA with a methylated cytosine-specific antibody (anti-5mC) or methylated cytosine binding protein, targeting the above-mentioned cytosine residues. The procedure is commonly combined with a tiling microarray or high throughput sequencing, allowing analysis of comprehensive methylation pattern of DNA possible.

High-density tiling arrays provide a fast, relatively low-cost opportunity, and minimal processing of the resulting data in generating genome-wide methylation profiles compared to high-throughput sequencing. Additionally, this methodology has been refined and upgraded over time through years of experimental

results, it has been commonly used and is widely accepted as a reliable technique. Different array designs are commercially available for several species and CpG-island or promoter arrays are most commonly used. Yet, on the other hand, high throughput sequencing grants its user far more advanced and complex data, allowing for careful assessment and observation of minute details that could be overlooked in assays, though it likewise requires equally greater investment in both resources and time (taking ~10 days to complete). Clearly, both have their own merits and downfalls. Upon designing the experiment, one must carefully consider the needs of the experiment and choose accordingly.

In our case, we used Mouse Promoter 1.0R array provided by Affymetrix. This single array comprises over 4.6 million tiled probes to inspect over 28 000 mouse promoter regions. Specifically, probes consisting of 25-mer oligos are tiled, leaving a gap of ~10 bp between probes (average resolution of 35 bp). Each promoter region covers ~6 kb upstream through 2.5 kb downstream of 5′ transcription start sites and is selected from NCBI mouse genome assembly.

MeDIP-Chip involves several steps (Figure 18.1): DNA preparation and DNA shearing via sonicate lysis to lengths between 200 and 1000 bp. The purified genomic DNA, randomly fragmented by sonication, is incubated with the anti-5mC antibody. (Methyl-CpG binding domain of the MBD2 is also available for selective binding of methylated DNA.) DNA that has been sheared, but not treated with the antibody,

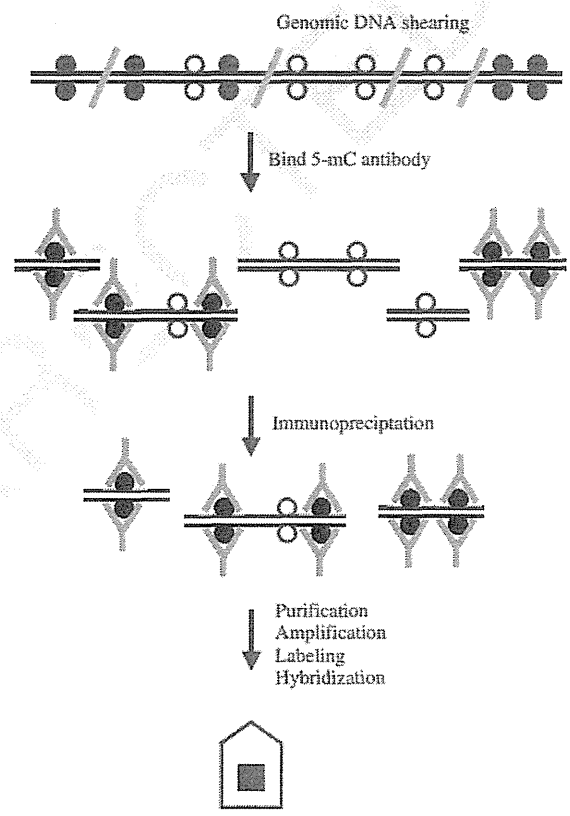

Figure 18.1 Procedure for MeDIP-chip

is used as the input sample. Afterwards, purified bound methylated DNA is amplified using random priming amplification. Amplified DNA is then fragmented and biotin-labeled based on the Affymetrix chromatin immunoprecipitation assay protocol, and probe DNA is hybridized to the tiling array. Data obtained from the array are then analyzed by Tiling Analysis Software (TAS; Affymetrix) and the Integrated Genome Browser (IGB; Affymetrix). IGB is an open source, desktop graphical display tool implemented in Java and provides view image of peaks of probe intensities (vertical bars), arrayed by chromosomal position (Nicol *et al.*, 2009). The image of the data obtained from chromosome 1 is shown in Figure 18.2. Each peak represents log-transformed intensities of the MeDIP sample versus the non-ChIP (chromatin immunoprecipitation) input control values (−log (*p*-value)), which is calculated using the Wilcoxon signed rank test. For example, in the series of the experiment, we find that the methylation level of gene A is lower than that of the control (Figure 18.3). As described earlier, the methylation of CpG islands associated with genes can have a direct effect on gene expression, and the cDNA microarray can be useful for analyzing such correlations. On this point, the RNA expression level of the "gene A" in the neonatally DES-exposed group shows threefold higher than that of the control, indicating a correlation between DNA methylation and mRNA expression. Therefore, combination of MeDIP-chip and cDNA microarray takes advantage of epigenetic status and the following gene expression changes.

It was reported that DNA methylation changes could induce transgenerational effects, further exacerbating the potential role of EDCs that affect this pathway (Anway *et al.*, 2005). The pups of prenatally DES-exposed mice have a higher risk of reproductive organ abnormalities including tumors (Newbold *et al.*, 1998, 2000). Disregulation of DNA methylation pattern by EDCs can explain such transgenerational effects if altered methylation takes place in the germ cells. Thus, information on long-term effects on gene memory in the DNA is needed. Using high-throughput microarrays to interrogate DNA methylation on a

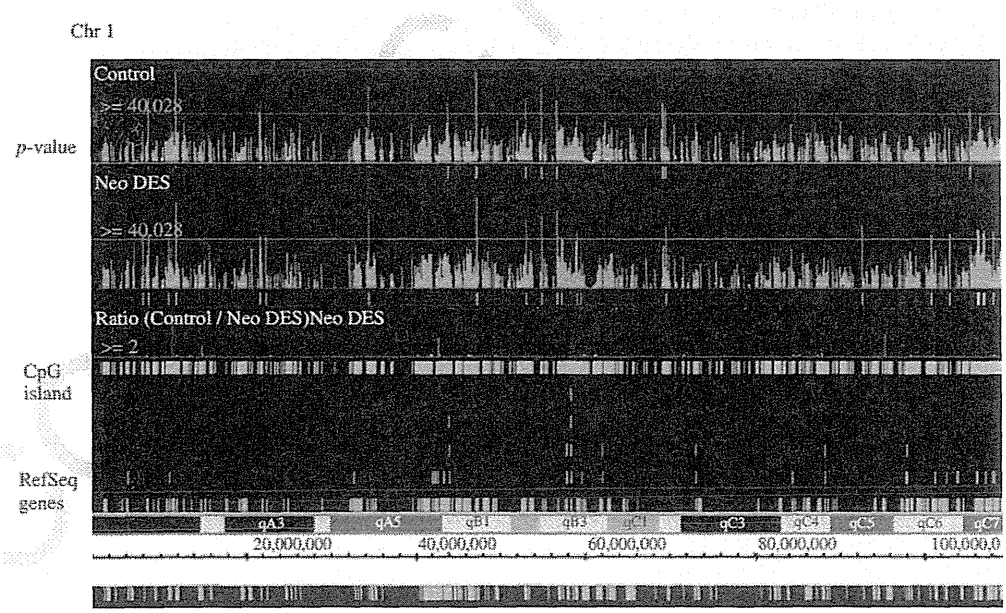

Figure 18.2 *Viewing of methylated DNA region on chromosome 1. Control: vagina from 10-week-old mouse ovariectomized two weeks before sacrifice. neoDES: vagina from 10-week-old neonatally DES-exposed mouse ovariectomized two weeks before sacrifice*

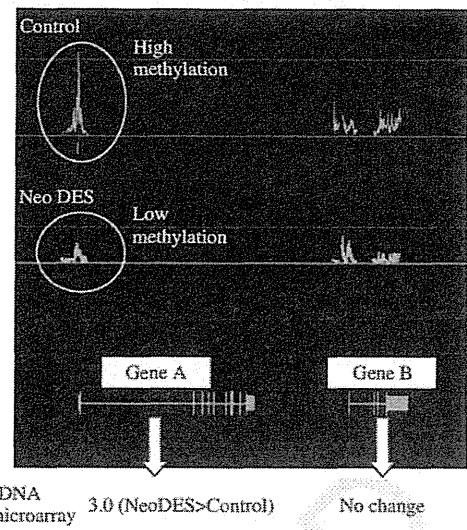

Figure 18.3 *The representative data showing correlation between DNA methylation and mRNA expression*

genome-wide level is an exciting research area that could yield important insights into many biological issues. On the other hand, the MeDIP-Chip method only allows the measurement of relative methylation differences between samples. To obtain an estimate on the general accuracy of the results from MeDIP-Chip analysis, several regions of interest should be validated with a second independent method. Variations of bisulfite sequence analyses offer the opportunity to examine a number of CpGs simultaneously.

18.4 Future research needs

EDCs interact with steroids, arylhydrocarbons, retinoids, and other nuclear receptors to regulate gene expression. Therefore, receptor-based functional assays are used as screening assays to detect biological activity of environmental chemicals. We need to understand the timing of gene expression (critical developmental window), the degree of gene expression (versus exposure dose of chemicals) in specific organs, degradation of chemicals, and normal range of various biomarkers. On the other hand, potentially new mechanisms of EDCs, action of genome-wide effects on DNA methylation status have also recently been postulated, and must be taken into consideration.

An emerging paradigm, the developmental origins of health and disease (DOHaD) or fetal origins of adult disease (FOAD) is a concept for considering the effects of EDCs on human and animal health (Gluckman and Hansen, 2005, 2006). The fundamental assumption of DOHaD is that the early developing period is susceptible to exogenous factors and it becomes a part of the risk of disease in later stages. One example of DOHaD is the DES syndrome and prenatally DES-exposed mouse model, as described previously. Remarkably, DES affects not only reproductive organ development and cancer formation, but also adipogenesis and obesity (Newbold *et al.*, 2007). Many obesogens, defined as chemicals that promote obesity by increasing the number of fat cells or the storage of fat, have been identified. Estrogens such as DES and genistein, organotins such as tributyltin, and bisphenol A are also known to be obesogenic in rodents when they are treated in developing periods (Newbold, Padilla-Banks, and Jefferson, 2009; Grün

et al., 2006; Rubin *et al.*, 2001). In human epidemiological studies reveal that in utero fetal nutritional status is a potential risk factor for obesity and related diseases (Barker *et al.*, 1990, 1993, Lucas, 1998). Plausible mechanisms include imprinting of obesity-sensitive hormonal pathways or changes in cell type and number, for example, adipocytes, established during development (Iguchi *et al.*, 2008). Search for the consequences on the developing exposure must be stringent; in particular, focus on the epigenetic effects is needed.

The availability of genomic information about non-model organisms is limited, and the toxicological approach has been extended to the field of wildlife zoology. Various modes of action of chemicals and nontraditional targets of EDCs have been recently summarized; however, understanding the toxicology and the molecular biology of the effects of EDCs on various species, from invertebrates to mammals, is still vitally important. The application of toxicogenomics to a variety of organisms (ecotoxicogenomics) could be a powerful tool for evaluating the effects of chemicals on ecosystems. Through systematic efforts to generate mechanistic information, diagnostic and predictive assessments of the risk of EDCs and toxic chemicals can be established in model species for ecological risk assessment.

Acknowledgments

This study was partially supported by the Grants-in-Aid from the Ministry of Health, Labor, and Welfare, Japan and Grants-in-Aid for Scientific Research from the Ministry of Education, Culture, Sports, Science, and Technology, Japan.

References

Anway, M.D., Cupp, A.S., Uzumcu, M., and Skinner, M.K. (2005) Epigenetic transgenerational actions of endocrine disruptors and male fertility. *Science*, **308**, 1466–1469.

Barker, D.J., Bull, A.R., Osmond, C., and Simmonds, S.J. (1990) Fetal and placental size and risk of hypertension in adult life. *Br. Med. J.*, **301**, 259–262.

Barker, D.J., Martyn, C.N., Osmond, C. *et al.* (1993) Growth in utero and serum cholesterol concentrations in adult life. *Br. Med. J.*, **307**, 1524–1527.

Block, K., Kardana, A., Igarashi, P., and Taylor, H.S. (2000) In utero diethylstilbestrol (DES) exposure alters Hox gene expression in the developing mullerian system. *FASEB J.*, **14**, 1101–1108.

Bromer, J.G., Wu, J., Zhou, Y., and Taylor, H.S. (2009) Hypermethylation of homeobox A10 by in utero diethylstilbestrol exposure: an epigenetic mechanism for altered developmental programming. *Endocrinology*, **150**, 3376–3382.

Gluckman, P. and Hansen, M. (2005) *The Fetal Matrix. Evolution, Development and Disease*, Cambridge University Press.

Gluckman, P. and Hansen, M. (eds) (2006) *Developmental Origins of Health and Disease*, Cambridge University Press.

Grün, F., Watanabe, H., Zamanian, Z. *et al.* (2006) Endocrine-disrupting organotin compounds are potent inducers of adipogenesis in vertebrates. *Mol. Endocrinol.*, **20**, 2141–2155.

Herbst, A.L., Ulfelder, H., and Poskanzer, D.C. (1971) Adenocarcinoma of the vagina. Association of maternal stilbestrol therapy with tumor appearance in young women. *N. Engl. J. Med.*, **284**, 878–881.

Ho, S.M., Tang, W.Y., Belmonte de Frausto, J., and Prins, G.S. (2006) Developmental exposure to estradiol and bisphenol A increases susceptibility to prostate carcinogenesis and epigenetically regulates phosphodiesterase type 4 variant 4. *Cancer Res.*, **66**, 5624–5632.

Iguchi, T., Watanabe, H., Ohta, Y., and Blumberg, B. (2008) Developmental effects: oestrogen-induced vaginal changes and organotin-induced adipogenesis. *Int. J. Androl.*, **31**, 263–268.

Jones, P.A. and Baylin, S.B. (2002) The fundamental role of epigenetic events in cancer. *Nat. Rev. Genet.*, **3**, 415–428.

Kato, S., Endoh, H., Masuhiro, Y. *et al.* (1995) Activation of the estrogen receptor through phosphorylation by mitogen-activated protein kinase. *Science*, **270**, 1491–1494.

Li, S., Hansman, R., Newbold, R. *et al.* (2003) Neonatal diethylstilbestrol exposure induces persistent elevation of c-fos expression and hypomethylation in its exon-4 in mouse uterus. *Mol. Carcinog.*, **38**, 78–84.

Li, S., Washburn, K.A., Moore, R. *et al.* (1997) Developmental exposure to diethylstilbestrol elicits demethylation of estrogen-responsive lactoferrin gene in mouse uterus. *Cancer Res.*, **57**, 4356–4359.

Lucas, A. (1998) Programming by early nutrition: an experimental approach. *J. Nutr.*, **128**, 401S–406S.

Ma, L., Benson, G.V., Lim, H. *et al.* (1998) Abdominal B (AbdB) Hoxa genes: regulation in adult uterus by estrogen and progesterone and repression in mullerian duct by the synthetic estrogen diethylstilbestrol (DES). *Dev. Biol.*, **197**, 141–154.

McLachlan, J.A., Newbold, R.R., and Bullock, B.C. (1980) Long-term effects on the female mouse genital tract associated with prenatal exposure to diethylstilbestrol. *Cancer Res.*, **40**, 3988–3999.

Miller, C., Degenhardt, K., and Sassoon, D.A. (1998) Fetal exposure to DES results in de-regulation of Wnt7a during uterine morphogenesis. *Nat. Genet.*, **20**, 228–230.

Miyagawa, S., Katsu, Y., Watanabe, H., and Iguchi, T. (2004a) Estrogen-independent activation of erbBs signaling and estrogen receptor alpha in the mouse vagina exposed neonatally to diethylstilbestrol. *Oncogene*, **23**, 340–349.

Miyagawa, S., Suzuki, A., Katsu, Y. *et al.* (2004b) Persistent gene expression in mouse vagina exposed neonatally to diethylstilbestrol. *J. Mol. Endocrinol.*, **32**, 663–677.

Newbold, R.R. (2004) Lessons learned from perinatal exposure to diethylstilbestrol. *Toxicol. Appl. Pharmacol.*, **199**, 142–150.

Newbold, R.R., Hanson, R.B., Jefferson, W.N. *et al.* (1998) Increased tumors but uncompromised fertility in the female descendants of mice exposed developmentally to diethylstilbestrol. *Carcinogenesis*, **19**, 1655–1663.

Newbold, R.R., Hanson, R.B., Jefferson, W.N. *et al.* (2000) Proliferative lesions and reproductive tract tumors in male descendants of mice exposed developmentally to diethylstilbestrol. *Carcinogenesis*, **21**, 1355–1363.

Newbold, R.R., Padilla-Banks, E., and Jefferson, W.N. (2009) Environmental estrogens and obesity. *Mol. Cell Endocrinol.*, **304**, 84–89.

Newbold, R.R., Padilla-Banks, E., Snyder, R.J., and Jefferson, W.N. (2007) Perinatal exposure to environmental estrogens and the development of obesity. *Mol. Nutr. Food Res.*, **51**, 912–917.

Nicol, J.W., Helt, G.A., Blanchard, S.G. Jr. *et al.* (2009) The integrated genome browser: free software for distribution and exploration of genome-scale datasets. *Bioinformatics*, **25**, 2730–2731.

Palmer, J.R., Wise, L.A., Hatch, E.E. *et al.* (2006) Prenatal diethylstilbestrol exposure and risk of breast cancer. *Cancer Epidemiol. Biomarkers Prev.*, **15**, 1509–1514.

Rubin, B.S., Murray, M.K., Damassa, D.A. *et al.* (2001) Perinatal exposure to low doses of bisphenol A affects body weight, patterns of estrous cyclicity, and plasma LH levels. *Environ. Health Perspect.*, **109**, 675–680.

Takasugi, N., Bern, H.A., and Deome, K.B. (1962) Persistent vaginal cornification in mice. *Science*, **138**, 438–439.

Tang, W.Y., Newbold, R., Mardilovich, K. *et al.* (2008) Persistent hypomethylation in the promoter of nucleosomal binding protein 1 (Nsbp1) correlates with overexpression of Nsbp1 in mouse uteri neonatally exposed to diethylstilbestrol or genistein. *Endocrinology*, **149**, 5922–5931.

Taylor, H.S., Arici, A., Olive, D., and Igarashi, P. (1998) HOXA10 is expressed in response to sex steroids at the time of implantation in the human endometrium. *J. Clin. Invest.*, **101**, 1379–1384.

Watanabe, H., Suzuki, A., Kobayashi, M. *et al.* (2003a) Similarities and differences in uterine gene expression patterns caused by treatment with physiological and non-physiological estrogens. *J. Mol. Endocrinol.*, **31**, 487–497.

Watanabe, H., Suzuki, A., Kobayashi, M. *et al.* (2003b) Analysis of temporal changes in the expression of estrogen-regulated genes in the uterus. *J. Mol. Endocrinol.*, **30**, 347–358.

Watanabe, H., Suzuki, A., Mizutani, T. *et al.* (2002) Genome-wide analysis of changes in early gene expression induced by oestrogen. *Genes. Cells*, **7**, 497–507.

Wu, Y., Halverson, G., Basir, Z. *et al.* (2005) Aberrant methylation at HOXA10 may be responsible for its aberrant expression in the endometrium of patients with endometriosis. *Am. J. Obstet. Gynecol.*, **193**, 371–380.

Yoshida, H., Broaddus, R., Cheng, W. *et al.* (2006) Deregulation of the HOXA10 homeobox gene in endometrial carcinoma: role in epithelial-mesenchymal transition. *Cancer Res.*, **66**, 889–897.